ORIGINAL ARTICLE

Effects of CPAP therapy withdrawal on exhaled breath pattern in obstructive sleep apnoea

Esther I Schwarz,[1] Pablo Martinez-Lozano Sinues,[2] Lukas Bregy,[2] Thomas Gaisl,[1] Diego Garcia Gomez,[2] Martin T Gaugg,[2] Yannick Suter,[2] Nina Stebler,[1] Yvonne Nussbaumer-Ochsner,[1] Konrad E Bloch,[1,3,4] John R Stradling,[5] Renato Zenobi,[2] Malcolm Kohler[1,3,4]

ABSTRACT

Background Obstructive sleep apnoea (OSA) is highly prevalent and associated with cardiovascular and metabolic changes. OSA is usually diagnosed by polysomnography which is time-consuming and provides little information on the patient's phenotype thus limiting a personalised treatment approach. Exhaled breath contains information on metabolism which can be analysed by mass spectrometry within minutes. The objective of this study was to identify a breath profile in OSA recurrence by use of secondary-electrospray-ionization-mass spectrometry (SESI-MS).

Methods Patients with OSA effectively treated with CPAP were randomised to either withdraw treatment (subtherapeutic CPAP) or continue therapeutic CPAP for 2 weeks. Exhaled breath analysis by untargeted SESI-MS was performed at baseline and 2 weeks after randomisation. The primary outcome was the change in exhaled molecular breath pattern.

Results 30 patients with OSA were randomised and 26 completed the trial according to the protocol. CPAP withdrawal led to a recurrence of OSA (mean difference in change of oxygen desaturation index between groups +30.3/h; 95% CI 19.8/h,40.7/h, p<0.001) which was accompanied by a significant change in 62 exhaled features (16 metabolites identified). The panel of discriminating mass-spectral features allowed differentiation between treated and untreated OSA with a sensitivity of 92.9% and a specificity of 84.6%.

Conclusion Exhaled breath analysis by SESI-MS allows rapid and accurate detection of OSA recurrence. The technique has the potential to characterise an individual's metabolic response to OSA and thus makes a comprehensible phenotyping of OSA possible.

Trial registration number NCT02050425 (registered at ClinicalTrials.gov).

Key messages

What is the key question?

- The question was brought up whether a disease-specific breath profile of obstructive sleep apnoea (OSA) giving insight into the systemic and metabolic consequences of OSA can be detected by the novel approach of breath analysis using untargeted real-time mass spectrometry.

What is the bottom line?

- This randomised controlled trial is the first study providing data on metabolic breath-prints using untargeted real-time mass spectrometry in OSA and shows that real-time breath analysis by mass spectrometry allows accurate detection of untreated OSA within minutes.

Why read on?

- The findings of this study provide a basis for future research using the non-invasive approach of breath analysis allowing the identification of specific diseases such as OSA, novel disease mediators or markers that may serve as both diagnostic and therapeutic targets, and could be translated into clinical practice.

INTRODUCTION

Obstructive sleep apnoea (OSA) is a highly prevalent and underdiagnosed sleep-related breathing disorder commonly associated with daytime sleepiness, increased rate of accidents, vascular dysfunction and hypertension, adverse cardiovascular outcome and diverse metabolic changes.[1–6] The major biological mechanisms underpinning the association between OSA and its systemic pathophysiological consequences are thought to include apnoea-related intermittent hypoxia leading to increased oxidative stress and increased sympathetic activity and arousal-induced reflex sympathetic activation.[7]

The gold-standard diagnostic test for OSA is in-laboratory polysomnography. Alternatively, portable home monitoring devices can diagnose OSA with sufficient accuracy in subjects with a high pre-test probability for OSA. However, all sleep studies are time-consuming and costly, and sometimes inconclusive due to technical artefacts or impaired sleep in an unaccustomed environment. Moreover, usual measures of disease severity derived from sleep studies do not allow reliable differentiation between different phenotypes of OSA, that is, cannot identify subjects who are susceptible to metabolic, neurological and cardiovascular effects of OSA.

OSA can be effectively treated with nocturnal CPAP which abolishes apnoea and hypopnoea and thus prevents the pathophysiological consequences

▶ Additional material is published online only. To view please visit the journal online (http://dx.doi.org/10.1136/thoraxjnl-2015-207597).

[1]Department of Pulmonology and Sleep Disorders Centre, University Hospital of Zurich, Zurich, Switzerland
[2]Department of Chemistry and Applied Biosciences, Swiss Federal Institute of Technology, Zurich, Switzerland
[3]Centre for Integrative Human Physiology, University of Zurich, Zurich, Switzerland
[4]Zurich Centre for Interdisciplinary Sleep Research, University of Zurich, Zurich, Switzerland
[5]Oxford Centre for Respiratory Medicine and NIHR Oxford Biomedical Research Centre, Churchill Hospital, Oxford, UK

Correspondence to
Professor Malcolm Kohler, Chair Respiratory Medicine, Clinical Director, Department of Pulmonology and Sleep Disorders Centre, University Hospital of Zurich, Raemistrasse 100, Zurich CH-8091, Switzerland; malcolm.kohler@usz.ch

*EIS and PM-LS contributed equally to this paper.

Received 25 July 2015
Revised 10 November 2015
Accepted 16 November 2015
Published Online First 15 December 2015

To cite: Schwarz EI, Martinez-Lozano Sinues P, Bregy L, *et al*. *Thorax* 2016;**71**:110–117.

of OSA. Short-term CPAP therapy withdrawal, in patients hitherto compliant with CPAP, can be applied to efficiently investigate the effects of OSA recurrence on physiology.[4]

Exhaled breath contains biochemical information about metabolism and its alterations. Most of the numerous exhaled compounds in breath are not produced in the lungs but released along the blood–gas barrier during gas exchange. Metabolic alterations are reflected in perturbed metabolic profiles that may be used to support the diagnosis of diseases such as OSA. This hypothesis is supported by studies suggesting that sleep apnoea results in altered plasma metabolites.[8] The main drawback of traditional plasma-based metabolomic analyses is that these procedures are time-consuming and labour-intensive. Alternatively, the wealth of metabolic information contained in exhaled breath could be analysed using electronic sensors.[9 10] However, the poor chemical specificity of electronic sensors does not allow for structural elucidation of the molecules imparting such OSA-specific breath-prints, limiting the usefulness of this technology. In this study, an approach combining the analytical power of mass spectrometry with the speed and non-invasiveness of electronic sensors was for the first time applied in patients with OSA to provide a comprehensive analysis of exhaled breath metabolites in real time. This technique, dubbed secondary electrospray ionisation-mass spectrometry (SESI-MS), has shown promise in detecting a wide range of metabolites in breath and allows rapid screening of patients.[11–16]

The objective of the study was to answer the question whether there is a disease-specific profile of exhaled breath in patients with OSA applying untargeted mass spectrometry, which might be used to confirm the diagnosis and also provide insight into the pathophysiology of OSA and underlying disease mechanisms on a metabolic level.

METHODS

Trial design

Randomised controlled parallel group trial.

Subjects

Patients aged between 20 and 75 years with known moderate-to-severe OSA with an oxygen desaturation index (ODI) of >20/h at the time of diagnosis were eligible if they currently had an ODI of >20/h (≥4%-dips) during an ambulatory nocturnal pulse oximetry on the fourth night off CPAP, and were effectively treated with CPAP for >12 months[4 17] (see online supplementary file).

Sample size

Because a formal power calculation based on the primary outcome was not possible, sample size estimation was based on the assumption that a clinically relevant difference in ODI—reflecting the disease of interest—between therapeutic and subtherapeutic CPAP is 15/h (SD12).[4 17] Based on this assumption, power calculation indicated that 28 patients were required in total to not miss a clinically relevant difference in ODI with a power of 90% (α=0.05) (see online supplementary file).

Patient evaluation and follow-up

The study was conducted at the University Hospital Zurich and Swiss Federal Institute of Technology, Zurich, Switzerland. The first patient was recruited in February 2014 and the last patient follow-up was completed in August 2014. Patients with OSA effectively treated with CPAP were randomly assigned (allocation ratio 1:1) to one of the two treatment groups—either to continue therapeutic CPAP or to withdraw it by the use of a subtherapeutic device. Follow-up assessments were performed 2 weeks after randomisation. Allocation was determined by unsorted envelopes. A member of the team not involved in patient enrolment and outcome assessment generated the allocation sequence and prepared the CPAP devices. Patients remained blinded to allocation.

The study protocol was approved by the cantonal ethics committee of Zurich (KEK-ZH-Nr.2013-0536). The trial was conducted according to the Declaration of Helsinki and registered at ClinicalTrials.gov (NCT02050425). Written informed consent was obtained from participants before participation in the trial.

Sleep studies and CPAP devices

Home sleep studies using the ApneaLink Plus-device (ResMed, San Diego, USA) were performed the night before the baseline and the follow-up breath analysis. OSA severity was quantified by ODI (≥4%-dips). Recurrence of OSA was defined as an ODI of >15/h in the follow-up sleep study (see online supplementary file).

Primary outcome

The primary outcome was the change in exhaled breath pattern in response to CPAP withdrawal (exhaled breath pattern in OSA recurrence) and its diagnostic accuracy.

Real-time breath analysis was performed using SESI-MS[14] coupled to a quadrupole time-of-flight mass spectrometer (AB Sciex, Concord, Canada) (see online supplementary file).

Secondary outcome measures

Secondary outcomes were changes in ODI, relationship between change in breath signal intensity and ODI and the chemical identification of the compounds differentiating treated from untreated OSA (see online supplementary file).

Data analysis

Changes within and between groups were analysed by dependent and independent *t* test, respectively. In all cases, 5000 bootstrap samples were used to compute p values. Subsequent estimate of the false discovery rate for multiple hypothesis testing was performed by computing q values for each p value as instructed by Storey.[18] Statistical significance level was set to α<0.05. Pearson's linear correlation coefficient and 95% bootstrap CIs between changes in breath signal intensity and changes in ODI were computed. The most correlating features were subjected to principal component analysis (PCA). OSA prediction was accomplished in a leave-one-out-cross-validation (LOOCV) by feature selection and subsequent classification using a random forest classification algorithm.[19] The most discriminative features were used to compute hierarchical cluster analysis and multidimensional scaling of the proximity matrix.

Statistica (V6.0; StatSoft, Tulsa, USA) and Matlab (MathWorks, Natick, USA) were used for data analysis. Further details on data analysis procedures are described in the online supplementary file.

RESULTS

Trial profile and patient characteristics

The study flow is shown in figure 1. Thirty patients with moderate-to-severe OSA were randomly assigned to either continue therapeutic CPAP or to withdraw it by the use of a subtherapeutic CPAP device. Of the30 patients, 28 (14 in each treatment group) completed the study. One participant in each group was lost to follow-up: one patient randomised to

Figure 1 Consort diagram.

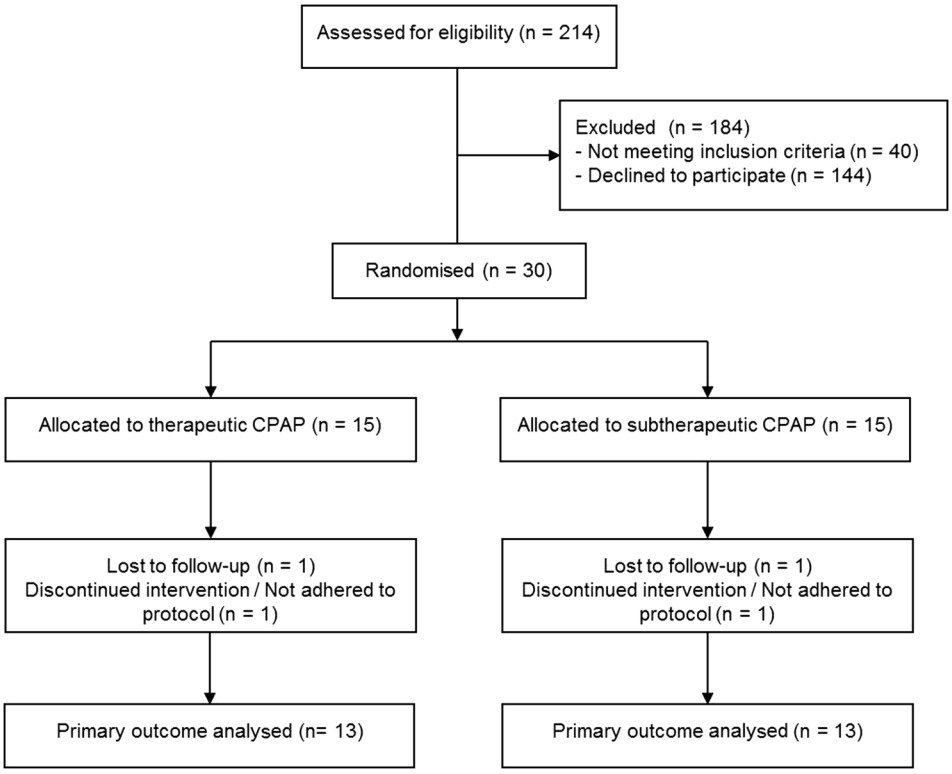

therapeutic CPAP did not show up to the follow-up visit and withdrew from the study due to personal reasons, and one subject allocated to subtherapeutic CPAP was lost to follow-up due to a relapse of a major depression requiring hospitalisation. Two subjects did not adhere to the protocol: one participant randomised to therapeutic CPAP experienced difficulties handling the provided CPAP device and did not use it consistently thus having relevant OSA at follow-up, and one participant randomised to subtherapeutic CPAP manipulated his sham device.

Table 1 Baseline patient characteristics

	Therapeutic CPAP (n=13)	CPAP-withdrawal (n=13)
Age, mean (SD), years	65.3±7.7	67.6±6.5
Male sex, n (%)	11 (85)	9 (69)
BMI, mean (SD), kg/m^2	32.8±5.4	34.4±6.2
Neck circumference, mean (SD), cm	44.2±3.4	40.2±3.4
Active smoker, n (%)	1 (8)	1 (8)
Former smoker, n (%)	3 (23)	8 (62)
Antihypertensive drugs, n (%)	5 (38)	9 (69)
Statins, n (%)	7 (54)	4 (31)
AHI at diagnosis, mean (SD), events per hour	55.3±22.6	45.8±16.4
ODI at diagnosis, mean (SD), events per hour	53.0±20.8	42.6±17.4
ESS at diagnosis, mean (SD), points	13.0±2.9	12.3±4.8
AHI on CPAP, mean (SD), events per hour	4.1±3.0	2.1±1.5
ESS on CPAP, mean (SD), points	5.1±2.2	6.5±2.5
CPAP compliance, mean (SD), hh:mm	06:50	07:08
FEV_1/FVC, mean (SD)	0.80 (0.04)	0.78 (0.02)
FVC, mean (SD), % predicted	90 (9)	95 (16)
FEV_1, mean (SD), % predicted	89 (13)	95 (16)

AHI, apnoea–hypopnoea-index; BMI, body mass index; ESS, Epworth Sleepiness Scale; ODI, oxygen desaturation-index.

Thus, the primary outcome was analysed in 26 patients who completed the trial per protocol. Baseline data are shown in table 1.

Effects of CPAP withdrawal on OSA

CPAP withdrawal was associated with return of OSA as evidenced by a significant increase in ODI (mean difference in change between groups, +30.3/h, 95% CI +19.8 to +40.7/h, p<0.001) (table 2).

Effects of CPAP withdrawal on exhaled breath

Exhaled breath pattern (primary outcome)

When compared with continuing CPAP, withdrawal of CPAP, and thus recurrence of OSA, was associated with altered exhaled breath patterns as determined by a statistically significant increase in 61 features and a decrease in 1 feature (see online supplementary table E1). Figure 2A–E shows one exemplary molecule which significantly increased in response to CPAP withdrawal. Online supplementary figure E3 shows additional examples of metabolites which allowed distinguishing between treated and untreated OSA. A blind prediction of OSA recurrence (defined as ODI >15/h) by a LOOCV using the 15 most-discriminating exhaled features in each cross-validation resulted in a sensitivity of 92.9% and specificity of 84.6% (table 3 and receiver operating characteristic (ROC) curve in figure 3A). The area under the ROC curve was 0.874 (95% CI 0.612 to 1). How these features discriminate the two groups is visualised in figure 3B, C.

Chemical identification of exhaled breath compounds

A comprehensive structural elucidation strategy allowed chemical identification of 22 molecules in the breath of patients with OSA (see eg, benzothiazole in figure 3D). Of the 22 identified molecules, 16 were shown to significantly change in response to CPAP withdrawal. These molecules are listed in table 4 (see also

Table 2 Outcomes from sleep studies

	Therapeutic CPAP (n=13)		Subtherapeutic CPAP (n=13)		Treatment effect		
	Baseline	follow-up	Baseline	Follow-up	Difference in change	95% CI	p Value
ODI	4.3 (3.2)	4.2 (1.7)	3.9 (3.5)	34.0 (16.3)	+30.3	+19.8 to +40.7	<0.001

Data are presented as means (SD).
ODI, oxygen desaturation index (4% dips).

online supplementary tables E1 and E3). Most of the identified molecules stem from a cluster of chemical families (eg, aldehydes). There is a strong association among the molecules within each chemical family (see figure 3E and online supplementary figure E6).

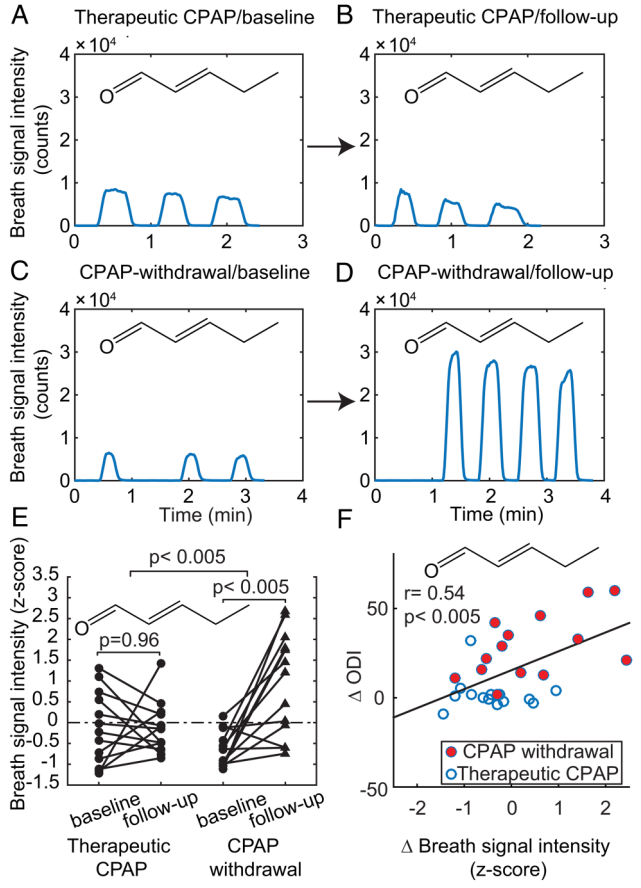

Figure 2 Pentenal in exhaled breath. Real-time breath analysis showing time traces of the signal intensity of one exemplary breath metabolite (pentenal) in a subject from the therapeutic CPAP and a subject from the CPAP-withdrawal group at baseline and at follow-up (A–D). The smoothed signals intensity traces increase during the exhalation cycles, providing good repeatability in signal intensity among the three to four replicate exhalations recorded within minutes. Signal intensity in the patient on therapeutic CPAP does not change from baseline (A) to follow-up (B) (7.4×10^3 to 5.7×10^3 counts). In contrast, the patient undergoing CPAP withdrawal showed a signal increase from 6×10^3 (C) counts at baseline to 2.7×10^4 (D) counts at follow-up (ie, 4.5-fold increase). Individual plots (E) of 2-pentenal in both groups (n=26) show significant breath compound enhancement. Correlation (F) is shown between changes in breath signal intensity of pentenal and changes in oxygen desaturation index (n=28) (r=0.54; 95% CI 0.2 to 0.78; p<0.003).

Association of breath signals with sleep apnoea severity

In addition to identification of metabolites changing in response to CPAP withdrawal, those showing a significant association between changes in signal intensity and disease severity were identified. Fifty-four features correlated significantly with changes in ODI as a measure of disease severity (see online supplementary table E2), including all 16 identified metabolites constituting the disease-specific breath profile (see figure 2F and online supplementary figure E4). The overall correlation of these compounds with disease severity is visualised in online supplementary figure E5 by reducing the significantly correlating features to one dimension using PCA.

DISCUSSION

This is the first study applying untargeted mass spectrometry to extract information from the exhaled breath metabolome in patients with OSA and paving the way for identifying a disease-specific breath profile. The use of the CPAP therapy withdrawal trial design enabled us to study OSA-specific breath patterns in a randomised controlled fashion, thus avoiding the possible biases of observational case–control studies.

The gold standard for OSA diagnosis, that is, in-laboratory polysomnography, is technically demanding and time-consuming. In addition, measures of OSA severity derived from sleep studies do not differentiate between distinct phenotypes of OSA, for example, symptomatic subjects or subjects with a pronounced increase in sympathetic activity or oxidative stress and thus increased vascular risk. For these reasons, a number of ongoing studies are attempting to define markers of sleep disorders at the protein and metabolic levels.[20 21] In contrast to blood and tissue specimens, exhaled breath carries easily accessible molecular markers, some of which are released along the blood–gas barrier and thus reflect changes in the blood and cell environment. It has been suggested that metabolites might move from different compartments into the blood and are then released via breath.[22]

Up to now there are only limited data in OSA derived from a small number of pilot studies on exhaled breath using electronic

Table 3 Diagnostic accuracy of exhaled breath analysis in OSA

	Predicted		
	OSA	No OSA	Total
Condition			
OSA	13	1	14
No OSA	2	11	13
Total	15	12	27

Confusion matrix of leave-one-out-cross-validation.
Summary of leave-one-out-cross-validation performance: correct prediction rate 88.9%; sensitivity 92.9%; specificity 84.6%; positive predictive value 86.7%; negative predictive value 91.7%; positive likelihood 6.036 and negative likelihood 0.084.
OSA, obstructive sleep apnoea defined by oxygen desaturation index ≥15/h.

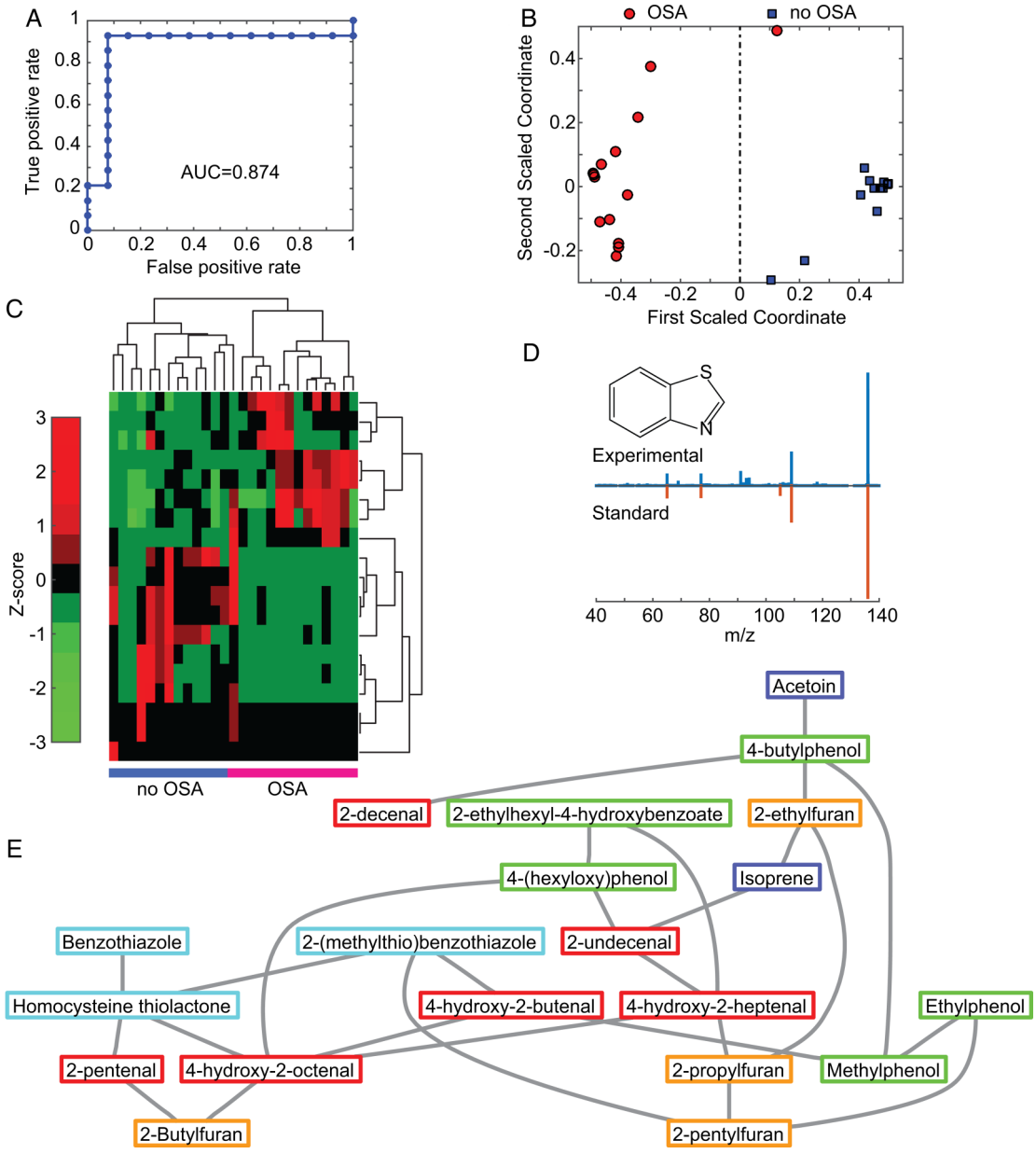

Figure 3 Obstructive sleep apnoea (OSA) prediction and metabolites identification are shown. (A) Receiver operating characteristic (ROC) curve obtained for OSA (ie, oxygen desaturation index (ODI)>15/h) prediction (n=27); (B) multidimensional scaling plot to the proximity matrix (n=27) computed using the most frequently selected features visualising two distinct groups are shown. (C) Similarly, hierarchical cluster analysis (n=27) revealed two distinct clusters; (D) head-to-tail fragmentation mass spectrum of benzothiazole found in breath (top) and the pure standard (bottom). (E) Visualisation of the associations of the identified metabolites. Interconnected metabolites are based on their partial correlations (requiring $p<0.01$). Compounds in red frames are a family of aldehydes; in yellow frames a series of furans; in green frames phenolic compounds; in light blue frames sulphur-containing compounds; in dark blue others.

sensors.[9 10] These studies have shown good discriminatory accuracy in OSA. However, electronic noses do not allow chemical analysis, limiting their use in elucidating pathophysiological mechanisms of diseases. State-of-the-art mass spectrometry has unparalleled chemical selectivity and sensitivity; however, most available commercial instruments were developed for offline analysis of liquid samples. Here we show that it is possible to take advantage of the powerful analytical capabilities of mass spectrometry, with minor hardware modifications that make instantaneous analysis of gas-phase metabolites in breath feasible. The used approach allows an immediate examination of breath with unparalleled chemical selectivity that (1) offers high diagnostic accuracy and at the same time (2) pinpoints the chemical structure of the exhaled molecules, with which a distinct metabolic fingerprint becomes recognisable. An additional natural advantage of examining metabolites in vivo is that any bias due to sample collection, storage and further manipulation is avoided. This is critical especially in the case of a gaseous sample such as breath.

In line with preliminary related work, we found that recurrence of OSA has a distinct altered metabolic breath profile. The technology used in this study can determine such metabolic breath profiles and make it available for detection of the disease (figure 3A–C) within minutes (<5 min/patient) (figure 2A–D). Our data suggest that some metabolites are augmented in the breath of patients with OSA and also correlate with disease

Table 4 Identified exhaled metabolites changing in response to recurrence of OSA

Breath signal features		Between-group changes (n=26)		
m/z	ID	p Value	q Value	95% CI
69.0681	Isoprene	0.020	0.15	0.15 to 2.23
97.0622	2-ethylfuran	0.022	0.16	0.12 to 2.14
102.0888	2-pentenal	0.002	0.15	0.55 to 2.55
109.0743	Methylphenol	0.002	0.15	0.58 to 2.57
111.0782	2-propylfuran	0.003	0.15	0.47 to 2.40
118.0288	Homocysteine thiolactone	0.019	0.15	0.14 to 2.08
123.0891	Ethylphenol	0.002	0.15	0.52 to 2.53
125.0930	2-Butylfuran	0.009	0.15	0.29 to 2.31
129.0885	4-hydroxy-2-heptenal	0.016	0.15	0.20 to 2.35
136.0193	Benzothiazole	0.026	0.17	0.08 to 2.01
139.1090	2-pentylfuran	0.004	0.15	0.44 to 2.51
155.1522	2-decenal	0.016	0.15	0.15 to 1.79
160.1298	4-hydroxy-2-octenal	0.019	0.15	0.17 to 2.38
166.0965	Mevalonic acid	0.032	0.17	0.04 to 1.70
182.0068	2-(methylthio)benzothiazole	0.020	0.15	0.13 to 1.99
196.1102	Digitalose	0.007	0.15	0.32 to 2.34

Of the 62 statistically significantly changing molecules, 16 were chemically identified. For more details (mean difference with CI), see online supplementary table E5.
OSA, Obstructive sleep apnoea.

severity (ie, ODI; see figure 2F and online supplementary figures E4 and E5). This suggests that these compounds may also be used to assess CPAP therapy effectiveness or compliance. Information derived from exhaled breath has the potential to characterise an individual's metabolic response to OSA which is important considering that to date, initiation of CPAP treatment mainly relies on symptoms and not on vascular risk, metabolic burden or comorbidities.

The fact that the most significant compounds identified belong to families of closely related molecules (eg, a homologous series of aldehydes) provides high confidence in the overall quality of the data obtained and implies that they are not raised merely by chance. This confidence is strengthened by the fact that the series of compounds for a given family correlate significantly with each other (see figure 3E and online supplementary figure E6). Most of the molecules identified here are known human metabolites related to different metabolic processes. For example a family of saturated aldehydes was significantly increased after CPAP withdrawal and correlate strongly with each other. Cell membrane lipid peroxidation leads to generation of various aldehydes. Subsequently, the released end-products may trigger different cellular events.[23] The closely related family of aldehydes found here reinforces the hypothesis of increased oxidative stress levels in OSA.[24] Isoprene, one of the identified discriminating molecules correlating with undecenal, is part of the mevalonic cycle (cholesterol synthesis).[25] Isoprene plays a role in sleep regulation and is increased in stressful conditions such as exercise, myocardial infarction and increased cardiac output.[26–31] Increased isoprene in the exhaled breath of patients with OSA may be due to increased sympathetic activity. Furthermore, isoprenoids serve as a base frame for steroids and thus cortisol, and also play a role in lipid metabolism that is altered possibly because of oxidative stress in OSA.[32]

Intriguingly, the family of aldehydes strongly correlates with a series of furans (see figure 3E and online supplementary figure E6). Furans have been found in the breath of healthy subjects. These compounds are related to smoking and are also thought to be secondary metabolites from the gut microbiome.[33 34] The number of former smokers in the CPAP withdrawal group was threefold higher than in the control group. However, this should not confound the finding of an increase in furans in the withdrawal group since it was only detected in response to CPAP withdrawal and was not present in the baseline breath analysis on therapeutic CPAP. The fact that only one participant in the withdrawal CPAP group was an active smoker suggests that the significant increase of alkyl furans in the CPAP withdrawal group is not related to active smoking but possibly to an altered gut flora in response to OSA recurrence, as found in a previous study.[8] Similarly, gut microbiota metabolites have been reported to be altered in sleep-deprived humans.[35] Along the same lines, intermittent hypoxia has been found to alter gut microbiota diversity in OSA mice models.[36] Moreover, we also found a family of phenols, including cresol, which is a unique bacterial metabolite from protein fermentation.[37] These metabolites are toxic bacterial end-products that, in the case of patients with compromised renal function, have been found to accumulate in the circulation, resulting in increased levels measurable in blood.[38] Another gut microbiome-related identified compound is acetoin.[34] Thus our data reinforce the notion that the altered metabolism associated with OSA may perturb the metabolic interplay between the gut flora and its host. In this regard, our findings add to the hypothesis that there is an association between gut microbiome composition and clinical phenotype.[39]

Another molecule found to be augmented in the breath of patients with OSA is benzothiazole and its closely related metabolite 2-(methylthio)benzothiazole. Benzothiazole has previously been reported in breath.[40] Interestingly, it has been found to be significantly increased in breath of patients with pulmonary arterial hypertension and cystic fibrosis.[41 42] It seems to correlate with pulmonary arterial pressure and pulmonary vascular resistance.[41] The fact that it is significantly increased following CPAP withdrawal suggests that apnoea-related nocturnal hypoxaemia indeed is associated with increased pulmonary arterial pressure. However, benzothiazole derivatives are widely used industrial products and have been reported to occur in the environment (eg, drinking water).[43] The reason why these exogenous compounds appear to be significantly altered in pulmonary hypertension, cystic fibrosis and OSA remains unknown. One hypothesis is that, as in the case of the toxic phenolic metabolites produced by gut bacteria, OSA could be associated with an impaired capacity to detoxify endogenous as well as exogenous small molecules, leading to an accumulation in blood and hence increased levels in breath. Another sulphur-containing molecule identified in the current study was homocysteine thiolactone, which has been associated with pathological conditions; for example, plasma levels have been linked with the development and progression of vascular complications in diabetic patients.[44] In summary, our data support the association of OSA with increased sympathetic activity, oxidative stress and perturbation of gut microbiota–host equilibrium.[7 24]

A possible limitation of our study is that the diagnostic accuracy of the OSA-specific exhaled breath pattern was not compared with polysomnography, which is considered the gold standard for diagnosis of OSA. Since this is a small sample of well-characterised patients, generalisability to other patients with OSA and a potential impact of comorbidities must be proven in future studies including more patients with OSA. As to the correlations found between breath signals and disease severity, one cannot completely exclude the possibility that the

correlations are to some extent due to differences between groups. However, correlations matrices show a significant overlap between both groups indicating that there are true correlations between changes in disease severity and exhaled features. Another possible limitation of the study is that the role of potential confounders not related to the disease—for example, increased caffeine intake because of increased sleepiness during the 2-week study period—cannot be determined. However, the applied short-term CPAP withdrawal model comparing treated and untreated patients with OSA is less prone to general confounding factors that do not change in the short term (eg, body mass index among many others). To avoid the anticipated influence of breathing manoeuvres on exhaled compounds[45] and to minimise artefacts,[46] breath analysis was highly standardised including a constant exhalation pressure.

The exhaled compounds changing in response to CPAP withdrawal cannot be considered as disease-specific markers of OSA without caution before they are validated in a population of untreated patients with OSA. Furthermore, in future studies, exhaled breath compounds should be compared with metabolomics of other body sources such as blood (hybrid metabolomics).[22]

Nevertheless, the possibility of identifying exhaled metabolites in real time and with high chemical selectivity is of general interest and makes this technique attractive for use in research and possibly in clinical practice. As such exhaled breath metabolomics can be applied for diagnostic goals, therapy guidance and monitoring, and to provide clues to underlying mechanisms.

In conclusion, real-time exhaled breath analysis by SESI-MS allows rapid and accurate detection of OSA recurrence. The technique has the potential to characterise an individual's metabolic response to OSA and thus makes a comprehensible phenotyping of OSA possible. However, to draw definite conclusions on diagnostic accuracy, the findings of this study have to be validated in an untreated OSA population.

Contributors Conception and design: MK, EIS, KEB, PM-LS, JRS and RZ. Data acquisition: EIS, LB, TG, DGG, NS and YN-O. Analysis and interpretation of data: PM-LS, EIS, DGG, MTG and YS. Drafting the article: EIS, PM-LS and MK. Revising the article for important intellectual content and final approval: all authors.

Funding This trial was supported by grants from the Swiss National Science Foundation (CR23I2_149617 and 32003B_143365/1), the University of Zurich Clinical Research Priority Program Sleep and Health and a Marie Curie European Reintegration Grant within the 7th European Community Framework Programme (276860).

Competing interests None declared

Ethics approval Cantonal Ethics Committee of Zurich.

Provenance and peer review Not commissioned; externally peer reviewed.

REFERENCES

1 Peppard PE, Young T, Barnet JH, *et al*. Increased prevalence of sleep-disordered breathing in adults. *Am J Epidemiol* 2013;177:1006–14.
2 Young T, Evans L, Finn L, *et al*. Estimation of the clinically diagnosed proportion of sleep apnea syndrome in middle-aged men and women. *Sleep* 1997;20:705–6.
3 George CF. Reduction in motor vehicle collisions following treatment of sleep apnoea with nasal CPAP. *Thorax* 2001;56:508–12.
4 Kohler M, Stoewhas AC, Ayers L, *et al*. Effects of continuous positive airway pressure therapy withdrawal in patients with obstructive sleep apnea: a randomized controlled trial. *Am J Respir Crit Care Med* 2011;184:1192–9.
5 Marin JM, Carrizo SJ, Vicente E, *et al*. Long-term cardiovascular outcomes in men with obstructive sleep apnoea-hypopnoea with or without treatment with continuous positive airway pressure: an observational study. *Lancet* 2005;365:1046–53.
6 Lévy P, Bonsignore MR, Eckel J. Sleep, sleep-disordered breathing and metabolic consequences. *Eur Respir J* 2009;34:243–60.
7 Kohler M, Stradling JR. Mechanisms of vascular damage in obstructive sleep apnea. *Nat Rev Cardiol* 2010;7:677–85.
8 Ferrarini A, Rupérez FJ, Erazo M, *et al*. Fingerprinting-based metabolomic approach with LC-MS to sleep apnea and hypopnea syndrome: a pilot study. *Electrophoresis* 2013;34:2873–81.
9 Benedek P, Lázár Z, Bikov A, *et al*. Exhaled biomarker pattern is altered in children with obstructive sleep apnoea syndrome. *Int J Pediatr Otorhinolaryngol* 2013;77:1244–7.
10 Greulich T, Hattesohl A, Grabisch A, *et al*. Detection of obstructive sleep apnoea by an electronic nose. *Eur Respir J* 2013;42:145–55.
11 Aernecke MJ, Mendum T, Geurtsen G, *et al*. Vapor pressure of Hexamethylene Triperoxide Diamine (HMTD) estimated using secondary electrospray ionization mass spectrometry. *J Phys Chem A* 2015;119:11514–22.
12 Zhu J, Bean HD, Jiménez-Díaz J, *et al*. Secondary electrospray ionization-mass spectrometry (SESI-MS) breathprinting of multiple bacterial lung pathogens, a mouse model study. *J Appl Physiol (1985)* 2013;114:1544–9.
13 Dillon LA, Stone VN, Croasdell LA, *et al*. Optimisation of secondary electrospray ionisation (SESI) for the trace determination of gas-phase volatile organic compounds. *Analyst* 2010;135:306–14.
14 Wu C, Siems WF, Hill HH, Jr. Secondary electrospray ionization ion mobility spectrometry/mass spectrometry of illicit drugs. *Anal Chem* 2000;72:396–403.
15 Martinez-Lozano Sinues P, Landoni E, Miceli R, *et al*. Secondary electrospray ionization-mass spectrometry and a novel statistical bioinformatic approach identifies a cancer-related profile in exhaled breath of breast cancer patients: a pilot study. *J Breath Res* 2015;9:031001.
16 Martinez-Lozano Sinues P, Meier L, Berchtold C, *et al*. Breath analysis in real time by mass spectrometry in chronic obstructive pulmonary disease. *Respiration* 2014;87:301–10.
17 Schwarz EI, Schlatzer C, Stehli J, *et al*. The effects of short-term CPAP withdrawal on myocardial perfusion in OSA—a randomised placebo-controlled trial. *Eur Respir J* 2014;44(Suppl 58): 4664.
18 Storey JD. A direct approach to false discovery rates. *J R Statist Soc B* 2002;64:479–98.
19 Breiman L. Random forests. *Mach Learn* 2001;45:5–32.
20 Feliciano A, Torres VM, Vaz F, *et al*. Overview of proteomics studies in obstructive sleep apnea. *Sleep Med* 2015;16:437–45.
21 Maeder MT, Strobel W, Christ M, *et al*. Comprehensive biomarker profiling in patients with obstructive sleep apnea. *Clin Biochem* 2015;48:340–6.
22 Broza YY, Mochalski P, Ruzsanyi V, *et al*. Hybrid volatolomics and disease detection. *Angew Chem Int Ed Engl* 2015;54:11036–48.
23 Rahman I. *Role of oxidative stress and inflammatory response in smokers and chronic obstructive pulmonary disease*. Oxidative Stress, Inflammation, and Health: CRC Press, 2005:291–368.
24 Lavie L. Oxidative stress inflammation and endothelial dysfunction in obstructive sleep apnea. *Front Biosci (Elite Ed)* 2012;4:1391–403.
25 Deneris ES, Stein RA, Mead JF. In vitro biosynthesis of isoprene from mevalonate utilizing a rat liver cytosolic fraction. *Biochem Biophys Res Commun* 1984;123:691–6.
26 DeMaster EG, Nagasawa HT. Isoprene, an endogenous constituent of human alveolar air with a diurnal pattern of excretion. *Life Sci* 1978;22:91–7.
27 Cailleux A, Allain P. Isoprene and sleep. *Life Sci* 1989;44:1877–80.
28 King J, Kupferthaler A, Frauscher B, *et al*. Measurement of endogenous acetone and isoprene in exhaled breath during sleep. *Physiol Meas* 2012;33:413–28.
29 Karl T, Prazeller P, Mayr D, *et al*. Human breath isoprene and its relation to blood cholesterol levels: new measurements and modeling. *J Appl Physiol* 2001;91:762–70.
30 Mendis S, Sobotka PA, Euler DE. Expired hydrocarbons in patients with acute myocardial infarction. *Free Radic Res* 1995;23:117–22.
31 Pabst F, Miekisch W, Fuchs P, *et al*. Monitoring of oxidative and metabolic stress during cardiac surgery by means of breath biomarkers: an observational study. *J Cardiothorac Surg* 2007;2:37.
32 Lavie L, Vishnevsky A, Lavie P. Evidence for lipid peroxidation in obstructive sleep apnea. *Sleep* 2004;27:123–8.
33 Ulanowska A, Kowalkowski T, Trawińska E, *et al*. The application of statistical methods using VOCs to identify patients with lung cancer. *J Breath Res* 2011;5:046008.
34 Garner CE, Smith S, de Lacy Costello B, *et al*. Volatile organic compounds from feces and their potential for diagnosis of gastrointestinal disease. *FASEB J* 2007;21:1675–88.
35 Weljie AM, Meerlo P, Goel N, *et al*. Oxalic acid and diacylglycerol 36:3 are cross-species markers of sleep debt. *Proc Natl Acad Sci USA* 2015;112: 2569–74.
36 Moreno-Indias I, Torres M, Montserrat JM, *et al*. Intermittent hypoxia alters gut microbiota diversity in a mouse model of sleep apnoea. *Eur Respir J* 2015;45:1055–65.
37 Hamer HM, De Preter V, Windey K, *et al*. Functional analysis of colonic bacterial metabolism: relevant to health? *Am J Physiol Gastrointest Liver Physiol* 2012;302: G1–9.
38 Evenepoel P, Meijers BKI, Bammens BRM, *et al*. Uremic toxins originating from colonic microbial metabolism. *Kidney Int* 2009;76:S12–19.

39 Le Chatelier E, Nielsen T, Qin J, *et al*. Richness of human gut microbiome correlates with metabolic markers. *Nature* 2013;500:541–6.
40 Phillips M, Herrera J, Krishnan S, *et al*. Variation in volatile organic compounds in the breath of normal humans. *J Chromatogr B Biomed Sci Appl* 1999;729:75–88.
41 Mansoor JK, Schelegle ES, Davis CE, *et al*. Analysis of volatile compounds in exhaled breath condensate in patients with severe pulmonary arterial hypertension. *PLoS ONE* 2014;9.
42 Robroeks CMHHT, van Berkel JJBN, Dallinga JW, *et al*. Metabolomics of volatile organic compounds in cystic fibrosis patients and controls. *Pediatr Res* 2010;68:75–80.
43 Asimakopoulos AG, Wang L, Thomaidis NS, *et al*. Benzotriazoles and benzothiazoles in human urine from several countries: a perspective on occurrence, biotransformation, and human exposure. *Environ Int* 2013;59:274–81.
44 Jakubowski H, Głowacki R. Chemical Biology of Homocysteine Thiolactone and Related Metabolites. Adv Clin Chem, 2011;55:81–103.
45 Sukul P, Trefz P, Schubert JK, *et al*. Immediate effects of breath holding maneuvers onto composition of exhaled breath. *J Breath Res* 2014;8:037102.
46 Thekedar B, Oeh U, Szymczak W, *et al*. Influences of mixed expiratory sampling parameters on exhaled volatile organic compound concentrations. *J Breath Res* 2011;5:016001.

Effects of CPAP therapy withdrawal on exhaled breath pattern in obstructive sleep apnoea

Esther I Schwarz*, Pablo Martinez-Lozano Sinues*, Lukas Bregy, Thomas Gaisl, Diego Garcia Gomez, Martin T Gaugg, Yannick Suter, Nina Stebler, Yvonne Nussbaumer-Ochsner, Konrad E Bloch, John R Stradling, Renato Zenobi, and Malcolm Kohler

*These authors contributed equally to this work

Supplementary File

Content

E-METHODS

Eligibility criteria

Patients aged between 20 and 75 years with known moderate to severe obstructive sleep apnoea (OSA), having an oxygen desaturation index (ODI) of >20/h at the time of diagnosis, registered in the database of the Sleep Disorders Center of the University Hospital Zurich were eligible if they currently had an ODI >20/h (≥4%-dips) during an ambulatory nocturnal pulse oximetry on the forth night off CPAP, were treated with CPAP for more than 12 months, and had a minimum CPAP-compliance of ≥4h/night as well as an apnoea-hypopnoea index (AHI) <10/h with treatment (according to CPAP machine download). Patients with previous ventilatory failure (awake SpO2 <93% and PaCO2>6kPa), unstable coronary or peripheral artery disease, severe arterial hypertension or hypotension (>180/110 or <90/60mmHg), Cheyne-Stokes breathing, acute inflammatory disease, any previous sleep-related accident or use of inhaled drugs, as well as professional drivers, were excluded.

Sample size

The sample size was estimated on the assumption that a clinically relevant difference in the secondary outcome ODI – reflecting the disease of interest – between therapeutic and subtherapeutic CPAP is 15/h (SD 12).[1-3] Based on this assumption, power calculation indicated that 28 patients are required in total to not miss a clinically relevant difference in the secondary outcome with a power of 90%, and a two-tailed significance level (alpha = 0.05). Taking into account a possible drop-out rate of approximately 6%, the total number of patients who had to be included was adjusted to 30 (15 patients in each arm).

Sleep studies and CPAP devices

Home sleep studies using the ApneaLink™ Plus device (ResMed Corp, San Diego, USA) were performed the night before the baseline and the follow-up breath-analysis. OSA severity was quantified by ODI (≥4%-dips). Data on treatment adherence were downloaded from the internal memory of the CPAP device. Recurrence of OSA was defined as an ODI>15/h in the follow-up sleep study.

After randomisation, patients received a ResMed S8 AutoSet Spirit II CPAP device (ResMed Corp, San Diego, CA, USA). Subtherapeutic pressure in the sham-device was achieved by setting the CPAP machine to the lowest pressure, insertion of a flow-restrictor at the machine outlet, and of extra holes in the collar of the tube at the end of the mask as previously described and validated.[1]

Experimental set-up of mass spectrometric breath analysis

Real-time breath analysis was performed with secondary electrospray ionisation-mass spectrometry (SESI-MS).[4-12] **Figure E1** shows a schematic of the SESI set-up used in this study. SESI-MS allows for real-time breath-printing by detection of both volatile and non-volatile trace components in breath without any sample pre-treatment. Only the last few seconds (typically around 6 sec.) of each exhalation were considered for analysis, thus excluding the initial part of the exhalation, which reflects mostly the dead space in the upper respiratory tract. Participants were examined in the fasting state and were asked to abstain from smoking, chewing gum, alcohol, tobacco, or caffeine on the day of the measurements. Room temperature and lighting were set at the same level for all measurements. Breathprints were collected in real-time in triplicate or quadruple. Participants exhaled three- or four-times through a disposable mouthpiece into a heated Teflon tube (50 cm long, 3 mm inner diameter) connected to the curtain gas port of a time-of-flight mass spectrometer (TripleTOF 5600, AB Sciex, Concord, ON, Canada). The sampling tube was surrounded with a heating tape at 90°C to prevent water condensation and to minimize losses of exhaled compounds onto the walls. While performing full exhalations, the subjects kept the pressure through the sampling line at 10 mbar (i.e. ~ 1 L/min)), as monitored by a digital manometer. A lab-built nano electrospray plume was used, where compounds of exhaled breath are ionised and subsequently mass analysed. Water (0.1% formic acid) was electrosprayed at a flow rate of 100 nl/min. The mass spectrometric breath signatures were subsequently analysed.

Mass spectra preprocessing

Figure E2 shows an overview of the procedure followed to deliver a final working matrix containing intensity values for mass spectrometric features for each of the 28 subjects that completed the trial analysed twice (i.e. baseline and follow-up). The 56 raw *.wiff mass spectra

were transformed to *.mzXML format using the online tool msConvert.[13] The *.mzXML files were imported into Matlab (R2014b). Each mass spectrum was interpolated (shape-preserving piecewise cubic interpolation method) in the range m/z 41-449 using a linearly spaced vector of $7x10^5$ points. The interpolated mass spectra for the 56 files were concatenated resulting in a matrix of 700,000 x 10,465 (m/z x scans). Each of the 10,465 spectra was mass calibrated using an iterative grid search algorithm. The algorithm aligns the spectrum to a set of reference peaks by scaling and shifting the domain such that the cross-correlation between the input signal and a synthetic target signal is maximal. The synthetic target signal was built with Gaussian pulses centered at the locations specified by the vector of reference peaks. After obtaining the new m/z scale, the algorithm computes the calibrated mass spectrum by shape-preserving piecewise cubic interpolation of the shifted input signal to the original m/z vector. As reference peaks we chose acetone (m/z 59.04914) and commonly present contaminants pthalic anhydride (m/z 149.02332), dibutylphthalate (m/z 279.15909) and polysiloxane (m/z 445.1201).[14] The calibrated mass spectra were then centroided (threshold=200 counts), resulting in 4,068 m/z values. To increase the signal/noise ratio, the peak intensities around +/- 0.002 m/z were summed. The centroiding procedure reduced the matrix to 4,068 x 10,465 (m/z x scans). Each of the 4,068 time traces were smoothed using a moving average filter (span = 5). In order to identify the signals rising during the exhalation maneuvers in each individual, we subjected the time traces for each of the 56 files to hierarchical cluster analysis. A total of 3,922 different signals were found in the breath of the entire study population. Further consideration was only given to the signals present in at least 11 subjects, reducing the data matrix to 2,504 x 10,465 (m/z x scans). To account for instrumental drift (e.g. detector sensitivity) across the eight months of measurements, the signals were normalized. Thus, the total ion current (TIC) for each of the 56 samples (typically 2,504 x ~200, m/z x scans) was computed. The median of the TIC signal during the three replicate exhalations was computed and the 2,504 x ~200 (m/z x scans) matrix was divided by this value. This process was done for the 56 sample matrices. Finally, the adjusted 2,504 x 10,465 (m/z x scans) matrix was multiplied by the median of the 56 TIC normalizing values to recover intensity values of the same order as the pre-normalized matrix. **Figure E2** shows the non-normalized TIC (blue trace) for 9 subjects (separated by dashed lines) and the normalized TIC (red trace). Finally, the replicate signal intensities at the plateau of the exhalation phase for each subject was averaged resulting in a matrix of 2,504 x 56 (m/z x subjects). The number of features was further reduced to 911 by excluding some redundant signals such as isotopic peaks. This 911 x 56 matrix was

finally autoscaled (i.e. z-score). The 56 columns corresponded to 14 patients on therapeutic CPAP measured twice (baseline and follow-up) and 14 patients on subtherapeutic CPAP measured twice (baseline and follow-up).

Statistical methods

Changes in exhaled breath pattern

The primary outcome, the mass spectrometric profile of exhaled breath pattern, was analysed by standard univariate and multivariate statistical methods. Since this is a pathophysiologic metabolomic study, only those patients that completed the trial per protocol (26/30) were used for between group comparisons (primary outcome: change in exhaled breath pattern). Between groups comparisons were performed using a two-sample t-test (two-sided; 5% significance level) using 5,000 bootstrap samples. Bootstrapping (i.e. sampling with replacement) is a non-parametric technique employed to account for distortions caused by the specific sample that may not be fully representative of the population, which can be the case for limited sample size [15]. Subsequent estimate of the false discovery rate for multiple hypothesis testing was performed by computing q-values for each p-value as instructed by Storey.[16] A cutoff value of $p < 0.05$ and $q < 0.2$ resulted in 108 significant features. The q-values were in the range of 0.15 for these 108 features, suggesting strong evidence that around 80 signals were indeed significantly altered after CPAP withdrawal. A closer inspection of the 108 significant features revealed that some of these peaks appertained to the same molecule (e.g. in-source fragments). Redundant features were removed and the 62 remaining ones are listed in **Table E1**. **Figure E3** shows the data for six of these molecules. Similarly to the between-group comparison, for the within-groups comparisons (baseline vs. follow-up), each of the 911 features was subjected to a t-test with 5,000 bootstrap samples. Subsequently, q-values were computed for both groups.[16] **Table E1** lists the within-groups p- and q-values, as well as 95% confidence intervals for the 62 significant features selected in the between-group comparisons.

Correlation between ODI and breath signals

The 28 patients completing the trial and thus providing complete data from baseline to follow-up were used for correlation analysis between changes in signal intensity of exhaled breath compounds and disease severity. Pearson's linear correlation coefficient between changes in

breath signals and changes in ODI for the 28 subjects was computed for the 911 features. Thus, the baseline breath signals were subtracted to the follow-up ones for both groups; p-values for testing the hypothesis of no correlation against the alternative that there is a nonzero correlation were computed simultaneously. 131 features were found to correlate significantly ($p < 0.05$) with ODI. In addition, 95% bootstrap confidence intervals were computed using 10,000 bootstrap samples. Only the features not containing 0 in the 95% confidence interval were further considered, reducing the number of features to 96. To further retain features with high confidence level, the leverage for the dataset was computed to exclude artificially high correlations due to outliers. Thus, if any point in the data set had a leverage value greater than 0.5, the correlation was not further considered. This final step reduced the number of features to 79. Similarly to the groups comparison described above, some of these features were found to be redundant (i.e. more than one feature per molecule). As a result, 54 features were left. **Table E2** lists the molecules suggesting a correlation between change in ODI and change in signal intensity. **Figure E4** displays eight examples. For easier visualization, the 79 features with the strongest correlation were subjected to principal component analysis (PCA). **Figure E5** shows the significant ($r = 0.59$; $p < 0.001$) correlation between the first principal component score and change in ODI.

OSA prediction

OSA prediction was accomplished in a leave-one-out-cross-validation (LOOCV) by feature selection and subsequent classification using a random forest classification algorithm.[17] It is important to note that to prevent any bias, the predicted sample was out of the training set (n= 26) at all time during the feature selection process, meaning that feature selection was also subjected to cross-validation.[18] In order to avoid unbalanced groups and thus making it cost-sensitive and unstable due to the limited sample size, two balanced groups were created by selecting the most extreme cases in terms of ODI.[19] Thus samples with ODI>15/h were labeled as “OSA” (n=14) and ODI<3 ‘no OSA’ (n=13). Prediction was computed using an ensemble of 200 decision trees using the top 15 most informative features. First an ensemble with 200 bagged decision trees was created for the training set. Predictor importance was estimated by ranking the variables according to their Gini score. The top 100 selected features were further used in a subsequent ensemble. A further feature selection over the 100 pre-selected variables was done by measuring the increase in prediction error if the values of that variable were permuted across the out-of-bag observations. Predictions for the test sample (n=1) were finally computed using the top 15 most

informative features. This process was repeated for the 27 samples. A ROC curve was computed with the classification scores. We then computed its area under the curve and it 95% confidence interval using 10,000 bootstrap samples. **Table E3** lists the features selected during the LOOCV. In an attempt to visualize and cluster the samples using the most significant features identified during the classification, a hierarchical cluster analysis (average linkage and correlation distance) using the 19 top variables (i.e. selected > 5 times) was computed. The same 19 top variables were used to perform multidimensional scaling of the proximity matrix. A scatter plot of the first and second scaled coordinates (i.e. corresponding to the two largest eigenvalues) is shown in **figure 3b**.

Molecule identification by mass spectrometry

In order to carry out compound identification, the most significant m/z features found in the statistical analysis phase, were chemically analysed *a posteriori*. Fragmentation (i.e. MS/MS) experiments were performed with the same instrument (i.e. AB Sciex Tripletof5600+). Subjects were asked to breath into the instrument in the same way as during the full MS mode analysis to perform MS/MS analysis in real-time. Multiple reaction monitoring-like experiments were conducted with arbitrary collision energy of 30V +/- 15 V. These spectra were compared with those obtained from standards and from the MassBank database (massbank.jp) and with *in silico* MS/MS spectra obtained with MetFrag,[20] an open-source combinatorial fragmenter for identifying product ions from small organic compounds that heuristically analyses every possible fragment from chemical structure databases such as KEGG or PubChem. To gain confidence in the assignments, we conducted further real-time measurements in full MS mode using an LTQ Orbitrap mass spectrometer, which usually results in a mass accuracy below 2 ppm. This high mass accuracy, in addition to the analysis of the isotopic distribution, allowed for the assignment of a unique molecular formula for each peak with very high confidence. Finally, for further identification, exhaled breath condensate samples were collected using a customized device following the recommendations suggested by the ATS/ERS task force.[21] These samples were analysed by UHPLC-HRMS, a technique that allows identification of small molecules.[22] When available, retention times were compared with those obtained from standards. Combining all these measurements, a molecular identity was proposed for 22 molecules (**Table E4**). Thus, the identification of these structures was based on different parameters (numbered from 1 to 6) that

imply different levels or confidence. For example, the comparison with a standard MS/MS spectrum or whether the compound has been previously found in exhaled breath.

E-TABLES

Table E1

		Between-groups (n = 26)					Within-groups									
							CPAP-withdrawal (n=13)					Therapeutic CPAP (n=13)				
m/z	**Metabolite**	**p**	**q**	**mean difference (z-score)**	**95% CI**		**p**	**q**	**mean difference (z-score)**	**95% CI**		**p**	**q**	**mean difference (z-score)**	**95% CI**	
69.0681	Isoprene	0.020	0.16	1.19	0.15	2.23	0.00031	0.01	1.21	0.49	1.93	0.934	0.50	0.03	-0.81	0.86
71.0592		0.010	0.16	1.34	0.28	2.40	0.00041	0.01	1.24	0.51	1.98	0.804	0.50	-0.10	-0.93	0.74
80.0148		0.016	0.16	1.25	0.20	2.30	0.01156	0.05	1.10	0.13	2.08	0.623	0.50	-0.15	-0.67	0.38
80.0148		0.016	0.16	1.25	0.20	2.30	0.01156	0.05	1.10	0.13	2.08	0.623	0.50	-0.15	-0.67	0.38
81.0505		0.010	0.15	1.19	0.26	2.12	0.03413	0.10	0.53	0.03	1.03	0.166	0.48	-0.66	-1.50	0.18
91.0384		0.017	0.16	1.26	0.19	2.34	0.00105	0.02	1.18	0.29	2.06	0.817	0.50	-0.09	-0.80	0.62
92.04728		0.020	0.16	1.11	0.14	2.07	0.00025	0.01	1.22	0.56	1.89	0.773	0.50	0.12	-0.65	0.89
97.0261		0.033	0.18	1.01	0.04	1.98	0.00077	0.02	1.19	0.43	1.96	0.656	0.50	0.18	-0.49	0.86
97.0622	2-ethylfuran	0.023	0.17	1.13	0.12	2.14	0.00038	0.01	1.38	0.51	2.25	0.444	0.48	0.25	-0.36	0.87
99.0894		0.010	0.16	1.26	0.26	2.25	0.01044	0.05	1.18	0.22	2.14	0.729	0.50	-0.08	-0.51	0.35
102.0888	2-pentenal	0.002	0.15	1.55	0.55	2.55	0.00008	0.01	1.57	0.75	2.39	0.942	0.50	0.02	-0.65	0.68
104.0477		0.023	0.17	0.82	0.09	1.56	0.00293	0.02	1.08	0.46	1.70	0.524	0.48	0.26	-0.21	0.73
105.0514		0.031	0.18	1.06	0.06	2.07	0.00526	0.03	0.98	0.30	1.66	0.833	0.50	-0.08	-0.90	0.73
108.0094		0.009	0.15	1.26	0.28	2.23	0.00520	0.03	1.25	0.26	2.23	0.953	0.50	-0.01	-0.32	0.30
109.0079		0.006	0.15	1.23	0.32	2.13	0.00147	0.02	1.32	0.46	2.18	0.743	0.50	0.09	-0.32	0.51
109.023		0.014	0.16	1.13	0.20	2.06	0.00124	0.02	1.15	0.45	1.86	0.944	0.50	0.02	-0.67	0.71
109.0621		0.028	0.17	1.07	0.08	2.06	0.00612	0.04	1.08	0.15	2.01	0.954	0.50	0.01	-0.46	0.49
109.0743	Methylphenol	0.002	0.15	1.57	0.58	2.57	0.00001	0.00	1.45	0.75	2.16	0.760	0.50	-0.12	-0.89	0.65
110.0185		0.039	0.20	0.90	0.01	1.78	0.01276	0.05	0.97	0.32	1.61	0.851	0.50	0.07	-0.61	0.75
111.0782	2-propylfuran	0.003	0.15	1.43	0.47	2.40	0.00005	0.01	1.49	0.71	2.28	0.850	0.50	0.06	-0.59	0.71
111.0893		0.007	0.15	1.22	0.31	2.13	0.01368	0.05	1.09	0.28	1.90	0.644	0.50	-0.13	-0.65	0.39
117.0991		0.008	0.15	1.27	0.30	2.24	0.00545	0.03	1.12	0.39	1.86	0.681	0.50	-0.14	-0.86	0.57
118.0288	Homocysteine thiolactone	0.020	0.16	1.11	0.14	2.08	0.00104	0.02	1.03	0.35	1.71	0.852	0.50	-0.08	-0.85	0.69
120.0781		0.006	0.15	1.03	0.28	1.78	0.00020	0.01	1.31	0.77	1.84	0.493	0.48	0.28	-0.30	0.86

122.082		0.029	0.17	0.81	0.05	1.57	0.01279	0.05	0.94	0.30	1.59	0.735	0.50	0.13	-0.34	0.61
122.1018		0.014	0.16	1.20	0.21	2.19	0.00271	0.02	1.26	0.32	2.20	0.844	0.50	0.06	-0.40	0.51
123.0891	Ethylphenol	0.002	0.15	1.52	0.52	2.53	0.00183	0.02	0.97	0.29	1.65	0.211	0.48	-0.55	-1.36	0.26
124.0817		0.037	0.19	0.94	0.02	1.86	0.00200	0.02	1.00	0.38	1.63	0.879	0.50	0.06	-0.69	0.81
125.093	2-Butylfuran	0.009	0.15	1.30	0.29	2.31	0.00036	0.01	1.30	0.59	2.01	0.992	0.51	0.00	-0.79	0.79
125.1291		0.018	0.16	1.23	0.18	2.27	0.00196	0.02	1.20	0.39	2.01	0.929	0.50	-0.02	-0.78	0.73
127.0188		0.017	0.16	0.98	0.14	1.82	0.00238	0.02	1.21	0.51	1.90	0.511	0.48	0.23	-0.32	0.78
129.0885	4-hydroxy-2-heptenal	0.016	0.16	1.27	0.20	2.35	0.00332	0.02	1.22	0.29	2.14	0.847	0.50	-0.06	-0.72	0.60
131.0568		0.007	0.15	1.23	0.31	2.16	0.01144	0.05	1.08	0.19	1.97	0.619	0.50	-0.16	-0.56	0.25
134.0649		0.016	0.16	1.06	0.17	1.96	0.00927	0.04	1.02	0.49	1.55	0.893	0.50	-0.04	-0.83	0.74
135.0406		0.012	0.16	1.20	0.23	2.16	0.00171	0.02	1.23	0.43	2.04	0.906	0.50	0.04	-0.59	0.66
136.0193	Benzothiazole	0.027	0.17	1.05	0.08	2.01	0.00147	0.02	1.30	0.44	2.15	0.433	0.48	0.25	-0.30	0.80
136.0449		0.013	0.16	1.20	0.22	2.18	0.00187	0.02	1.22	0.39	2.04	0.950	0.50	0.01	-0.60	0.63
137.0544		0.008	0.15	1.15	0.27	2.03	0.00345	0.02	1.06	0.36	1.76	0.817	0.50	-0.09	-0.70	0.52
138.0144		0.005	0.15	1.26	0.35	2.17	0.00139	0.02	1.31	0.47	2.15	0.879	0.50	0.04	-0.42	0.51
138.0563		0.012	0.16	1.28	0.24	2.32	0.01539	0.05	0.92	0.08	1.76	0.358	0.48	-0.36	-1.07	0.35
139.109	2-pentylfuran	0.004	0.15	1.48	0.44	2.51	0.00007	0.01	1.45	0.66	2.25	0.939	0.50	-0.02	-0.77	0.73
143.1161		0.017	0.16	1.29	0.19	2.39	0.02435	0.08	0.89	0.07	1.71	0.272	0.48	-0.40	-1.22	0.42
147.0504		0.013	0.16	1.26	0.23	2.29	0.00326	0.02	1.15	0.24	2.05	0.743	0.50	-0.12	-0.72	0.49
149.0957		0.008	0.15	1.50	0.36	2.65	0.00543	0.03	1.12	0.23	2.01	0.250	0.48	-0.38	-1.19	0.44
150.0609		0.015	0.16	1.13	0.19	2.07	0.00367	0.03	1.08	0.40	1.76	0.880	0.50	-0.05	-0.78	0.67
150.1005		0.015	0.16	1.21	0.20	2.22	0.00931	0.04	1.03	0.15	1.92	0.624	0.50	-0.18	-0.77	0.41
152.0665		0.016	0.16	1.28	0.20	2.35	0.00975	0.04	0.68	0.07	1.28	0.213	0.48	-0.60	-1.56	0.36
154.0634		0.019	0.16	1.09	0.14	2.03	0.00298	0.02	1.11	0.34	1.89	0.931	0.50	0.03	-0.60	0.66
155.1522	2-decenal	0.017	0.16	0.97	0.15	1.79	0.00970	0.04	1.11	0.52	1.70	0.650	0.50	0.14	-0.50	0.78
158.123		0.036	0.19	1.24	0.04	2.45	0.00851	0.04	0.96	0.12	1.80	0.497	0.48	-0.28	-1.24	0.68
160.1298	4-hydroxy-2-octenal	0.019	0.16	1.27	0.17	2.38	0.01286	0.05	0.96	0.12	1.81	0.421	0.48	-0.31	-1.12	0.49
166.0965	Mevalonic acid	0.033	0.18	0.87	0.04	1.70	0.00465	0.03	0.94	0.26	1.62	0.874	0.50	0.06	-0.49	0.62
167.1031		0.037	0.19	1.25	0.03	2.47	0.00338	0.02	0.84	0.23	1.45	0.392	0.48	-0.41	-1.55	0.72
169.0865		0.027	0.17	1.21	0.10	2.32	0.00868	0.04	0.90	0.17	1.64	0.483	0.48	-0.31	-1.22	0.61

170.1106		0.003	0.15	1.54	0.51	2.57	0.00058	0.01	1.07	0.39	1.75	0.290	0.48	-0.47	-1.31	0.38
175.1086		0.033	0.18	1.11	0.05	2.16	0.00774	0.04	0.95	0.17	1.72	0.704	0.50	-0.16	-0.96	0.64
182.0068	2-(methylthio) benzothiazole	0.021	0.16	1.06	0.13	1.99	0.00565	0.03	1.15	0.46	1.83	0.782	0.50	0.09	-0.61	0.79
196.1102	Digitalose	0.008	0.15	1.33	0.32	2.34	0.00728	0.04	1.22	0.26	2.18	0.638	0.50	-0.11	-0.58	0.35
205.0704		0.013	0.16	-1.19	-2.15	-0.22	0.04613	0.11	-0.52	-1.00	-0.04	0.168	0.48	0.67	-0.23	1.57
209.1522		0.027	0.17	1.15	0.09	2.21	0.00391	0.03	0.95	0.29	1.61	0.648	0.50	-0.21	-1.11	0.70
221.1882		0.030	0.17	1.22	0.07	2.36	0.03879	0.10	0.79	-0.07	1.64	0.274	0.48	-0.43	-1.28	0.42
297.0996		0.029	0.17	1.12	0.08	2.17	0.03560	0.10	0.90	0.07	1.73	0.495	0.48	-0.22	-0.96	0.51

Table E1. Features significantly altered in response to CPAP-withdrawal.

Table E2

Correlation between changes of breath signals and changes of ODI (n = 28)					
m/z	ID	Pearson's correlation coefficient	95% CI		p
85.07397	2-pentenal	0.54	0.20	0.78	0.003
109.0743	Methylphenol	0.45	0.19	0.63	0.016
111.0782	propylfuran	0.40	0.08	0.65	0.033
118.0288	Homocysteine thiolactone	0.37	0.03	0.61	0.050
123.0891	Ethylphenol	0.49	0.20	0.68	0.008
123.1136		0.40	0.01	0.76	0.033
125.093	2-butylfuran	0.44	0.11	0.67	0.020
129.0885	4-hydroxy-2-heptenal	0.48	0.14	0.75	0.009
137.0544		0.44	0.18	0.65	0.019
139.109	2-pentylfuran	0.38	0.04	0.62	0.047
143.1045	4-hydroxy-2-octenal	0.42	0.05	0.70	0.025
152.0665		0.42	0.15	0.61	0.027
155.1522	2-decenal	0.41	0.07	0.66	0.029
160.1298	4-hydroxy-2-octenal	0.42	0.11	0.67	0.025
164.0716		0.41	0.06	0.78	0.030
166.0965	Mevalonic acid	0.40	0.10	0.62	0.034
169.1559	2-undecenal	0.38	0.04	0.70	0.046
170.1106		0.38	0.08	0.62	0.043
182.0837		0.38	0.11	0.60	0.045
195.1333	Hexyloxy-phenol	0.38	0.04	0.65	0.049
196.1102	Digitalose	0.59	0.18	0.84	0.001
199.0722		0.53	0.26	0.83	0.003
207.1338		0.38	0.12	0.57	0.049
209.1131		0.40	0.13	0.59	0.035
210.15		0.39	0.04	0.69	0.038
211.1263		0.38	0.06	0.61	0.044
213.0183		0.51	0.13	0.83	0.005
221.1492		0.38	0.13	0.57	0.044
223.128		0.44	0.13	0.72	0.018
227.124		0.43	0.14	0.65	0.024
233.149		0.41	0.12	0.60	0.030
236.0837		-0.39	-0.59	-0.07	0.038
236.9662		0.41	0.07	0.75	0.028
237.1066		0.40	0.18	0.57	0.037
243.1177		0.38	0.13	0.59	0.046
247.1633		0.46	0.14	0.68	0.014
249.0022		0.42	0.08	0.76	0.025
249.1438		0.38	0.18	0.57	0.046
249.1788		0.45	0.18	0.62	0.017
251.1605	2-ethylhexyl-4-hydroxybenzoate	0.43	0.09	0.68	0.023

256.9903	0.42	0.06	0.75	0.028
257.0439	0.45	0.05	0.79	0.017
262.982	0.39	0.01	0.76	0.040
263.1219	0.43	0.18	0.65	0.023
263.1604	0.38	0.08	0.60	0.048
272.0379	0.38	0.12	0.64	0.046
278.2139	0.43	0.13	0.64	0.024
294.0233	0.40	0.03	0.72	0.035
303.0174	0.37	0.04	0.60	0.050
307.0065	0.42	0.11	0.73	0.025
309.0074	0.39	0.10	0.70	0.041
313.1119	0.40	0.08	0.76	0.034
315.054	0.38	0.05	0.65	0.046
369.0855	0.46	0.16	0.71	0.014

Table E2. Features correlating with disease severity (oxygen desaturation index).

Table E3

Features selected during leave-one-out-cross-validation (n = 27)											
m/z	Selection frequency	m/z	Selection frequency	m/z	Selection frequency	m/z	Selection frequency	m/z	Selection frequency	m/z	Selection frequency
183.0104	18	93.05505	4	127.0223	2	105.01	1	177.0047	1	258.9935	1
213.9602	18	139.109	4	129.0121	2	108.0094	1	182.9446	1	274.1205	1
262.982	16	168.9793	4	147.0504	2	109.0079	1	184.0036	1	276.998	1
213.9689	15	182.9463	4	151.9598	2	110.0185	1	188.1075	1	284.0285	1
53.03835	14	216.8669	4	164.9442	2	110.0652	1	195.9709	1	294.8603	1
319.9873	13	321.9836	4	165.1243	2	111.0053	1	196.1667	1	304.0584	1
258.9889	12	43.05457	3	167.9902	2	125.0137	1	196.9349	1	327.0772	1
112.0084	10	44.02562	3	175.1086	2	128.0673	1	198.9341	1	329.9979	1
221.9646	10	79.03848	3	194.9363	2	131.0568	1	205.9698	1	330.9917	1
258.9906	9	87.04228	3	210.1541	2	132.057	1	208.1747	1	331.0056	1
346.0183	9	90.07256	3	237.9716	2	134.1267	1	211.9936	1	358.1237	1
125.1291	8	92.04728	3	258.9423	2	136.0449	1	213.9806	1	393.2893	1
111.0782	7	97.06219	3	298.0392	2	138.0144	1	213.9847	1		
139.0122	7	102.0888	3	371.319	2	138.9994	1	213.9957	1		
182.0068	7	112.0183	3	57.03326	1	140.1418	1	216.0643	1		
213.9649	7	123.1148	3	58.06375	1	141.0103	1	221.9809	1		
319.9856	7	151.1094	3	62.9889	1	146.0893	1	228.0654	1		
123.1136	6	198.9318	3	69.06811	1	157.0097	1	228.0671	1		
333.0025	6	213.9887	3	71.04749	1	157.0237	1	231.1714	1		
81.02835	5	344.975	3	83.08351	1	160.0592	1	232.9579	1		
166.983	5	89.06946	2	95.04725	1	164.0267	1	240.9931	1		
222.9508	5	90.0714	2	97.05462	1	166.9987	1	248.9649	1		
321.9865	5	103.0913	2	98.06646	1	168.9863	1	250.0222	1		
337.012	5	109.023	2	101.0571	1	170.9867	1	250.9664	1		
88.04596	4	122.1018	2	103.0924	1	172.1104	1	250.9822	1		

Table E3. LOOCV selected features. The top 19 (i.e. selected at least 6 times) were used to generate figures 3b and 3c.

Table E4

TripleTOF m/z	Orbitrap m/z	Formula	Acc. / ppm	MS/MS-Fragments	ID	ID based on
69.0681	69.0698	C_5H_9	1.1	C_3H_5	Isoprene	4, 6
85.0740 102.0888	85.0648 102.0913	C_5H_9O C_5H_9O +NH_3	0.1	C_3H_7O, C_2H_3O	2-pentenal	2, 5
87.0423	87.0440	$C_4H_7O_2$	0.6	C_4H_5O, C_3H_7O, C_2H_3O	4-hydroxy-2-butenal	2, 5
89.0695	89.0595	$C_4H_9O_2$	2.3	C_4H_7O, C_2H_3O	Acetoin	4, 6
97.0622	97.0647	C_6H_9O	0.9	C_4H_5O	2-ethylfuran	1, 5, 6
109.0743	109.0649	C_7H_9O	1	C_7H_7, C_6H_7O, C_6H_5	Methylphenol	1, 5, 6
111.0782	111.0804	$C_7H_{11}O$	0.4	C_5H_7O, C_4H_5O	2-propylfuran	2, 5, 6
118.0288	118.0320	C_4H_8NOS	0.9	C_3H_8NS, C_3H_6NO, C_3H_6N	Homocysteine thiolactone	1, 5, 6
123.0891	123.0803	$C_8H_{11}O$	1.1	C_8H_9, C_6H_7O, C_6H_5	Ethylphenol	1, 4
125.0930	125.0961	$C_8H_{13}O$	0.1	C_6H_9O, C_4H_5O	2-Butylfuran	2, 5, 6
129.0885	129.0908	$C_7H_{13}O_2$	1.6	$C_7H_{11}O$, C_5H_9O, C_4H_7O, C_2H_3O	4-hydroxy-2-heptenal	2, 5, 6
136.0193	136.0215	C_7H_6NS	0.3	C_6H_5S, C_6H_5, C_3HS, C_5H_5	Benzothiazole	1, 5, 6
139.1090	139.1117	$C_9H_{15}O$	0.3	$C_7H_{11}O$, C_6H_9O, C_4H_5O	2-pentylfuran	1, 3, 5, 6
143.1045 160.1298	143.1066 160.1332	$C_8H_{15}O_2$ $C_8H_{15}O_2$ +NH_3	0.4 0.1	$C_8H_{13}O$, C_3H_5O, C_2H_3O	4-hydroxy-2-octenal	2, 5, 6
151.1094	151.1117	$C_{10}H_{15}O$	0.3	$C_{10}H_{13}$, $C_8H_{11}O$, C_7H_9O, C_6H_7O, C_6H_5	4-butylphenol	1, 4
155.1522	155.1430	$C_{10}H_{19}O$	0.3	$C_8H_{15}O$, C_2H_3O	2-decenal	2, 5, 6
166.0965	166.1075	$C_6H_{16}NO_4$	0.7	$C_6H_{13}O_4$, $C_4H_7O_2$, C_4H_9O	Mevalonic acid	4
169.1559	169.1588	$C_{11}H_{21}O$	0.6	C_2H_3O	2-undecenal	2, 5, 6
182.0068	182.0095	$C_8H_8NS_2$	1.3	$C_7H_5NS_2$, $C_6H_4S_2$, C_7H_5NS, C_6H_5NS, C_6H_5S, C_6H_4S, C_5H_4S, C_6H_5N, C_6H_5, C_5H_5	2-(methylthio)benzothiazole	1, 3, 4
195.1333	195.1381	$C_{12}H_{19}O_2$	0.7	$C_7H_5O_2$, C_6H_7O, C_6H_5	4-(hexyloxy)phenol	1, 3 4
196.1102	196.1177	$C_7H_{18}NO_5$	1.3	$C_7H_{15}O_5$, $C_7H_{13}O_4$, $C_3H_5O_2$, C_3H_7O	Digitalose	4
251.1605	251.1639	$C_{15}H_{23}O_3$	1.1	$C_{13}H_{19}O_3$, $C_{10}H_9O_3$, $C_8H_5O_3$, $C_7H_5O_2$, C_6H_5O	2-ethylhexyl-4-hydroxybenzoate	1, 3, 4

Table E4. Combination of different approaches (1-6) allowed chemical identification of 22 molecules in exhaled breath of OSA patients. 16 of the 22 two identified molecules were shown to significantly change in response to CPAP withdrawal. 1=Comparison with standard MS/MS

spectra. 2=Comparison with similar standard MS/MS spectra. 3=Retention time in UHPLC (standard vs. EBC). 4=Comparison with in silico MS/MS spectra (MetFrag – KEGG, score: 1.0). 5=Comparison with in silico MS/MS spectra (MetFrag–PubChem, score: 1.0). 6=Previously found in the volatilome database.[23 24]

Table E5

		Between-groups (n = 26)					Within-groups									
							CPAP-withdrawal (n=13)					Therapeutic CPAP (n=13)				
m/z	Metabolite	p	q	mean difference (z-score)	95% CI		p	q	mean difference (z-score)	95% CI		p	q	mean difference (z-score)	95% CI	
69.0681	Isoprene	0.02	0.16	1.19	0.15	2.23	0.00031	0.01	1.21	0.49	1.93	0.934	0.5	0.03	-0.81	0.86
97.0622	2-ethylfuran	0.023	0.17	1.13	0.12	2.14	0.00038	0.01	1.38	0.51	2.25	0.444	0.48	0.25	-0.36	0.87
102.0888	2-pentenal	0.002	0.15	1.55	0.55	2.55	0.00008	0.01	1.57	0.75	2.39	0.942	0.5	0.02	-0.65	0.68
109.0743	Methylphenol	0.002	0.15	1.57	0.58	2.57	0.00001	0	1.45	0.75	2.16	0.76	0.5	-0.12	-0.89	0.65
111.0782	2-propylfuran	0.003	0.15	1.43	0.47	2.4	0.00005	0.01	1.49	0.71	2.28	0.85	0.5	0.06	-0.59	0.71
118.0288	Homocysteine thiolactone	0.02	0.16	1.11	0.14	2.08	0.00104	0.02	1.03	0.35	1.71	0.852	0.5	-0.08	-0.85	0.69
123.0891	Ethylphenol	0.002	0.15	1.52	0.52	2.53	0.00183	0.02	0.97	0.29	1.65	0.211	0.48	-0.55	-1.36	0.26
125.093	2-Butylfuran	0.009	0.15	1.3	0.29	2.31	0.00036	0.01	1.3	0.59	2.01	0.992	0.51	0	-0.79	0.79
129.0885	4-hydroxy-2-heptenal	0.016	0.16	1.27	0.2	2.35	0.00332	0.02	1.22	0.29	2.14	0.847	0.5	-0.06	-0.72	0.6
136.0193	Benzothiazole	0.027	0.17	1.05	0.08	2.01	0.00147	0.02	1.3	0.44	2.15	0.433	0.48	0.25	-0.3	0.8
139.109	2-pentylfuran	0.004	0.15	1.48	0.44	2.51	0.00007	0.01	1.45	0.66	2.25	0.939	0.5	-0.02	-0.77	0.73
155.1522	2-decenal	0.017	0.16	0.97	0.15	1.79	0.0097	0.04	1.11	0.52	1.7	0.65	0.5	0.14	-0.5	0.78
160.1298	4-hydroxy-2-octenal	0.019	0.16	1.27	0.17	2.38	0.01286	0.05	0.96	0.12	1.81	0.421	0.48	-0.31	-1.12	0.49
166.0965	Mevalonic acid	0.033	0.18	0.87	0.04	1.7	0.00465	0.03	0.94	0.26	1.62	0.874	0.5	0.06	-0.49	0.62
182.0068	2-(methylthio) benzothiazole	0.021	0.16	1.06	0.13	1.99	0.00565	0.03	1.15	0.46	1.83	0.782	0.5	0.09	-0.61	0.79
196.1102	Digitalose	0.008	0.15	1.33	0.32	2.34	0.00728	0.04	1.22	0.26	2.18	0.638	0.5	-0.11	-0.58	0.35

E-FIGURES

Figure E1

Top View

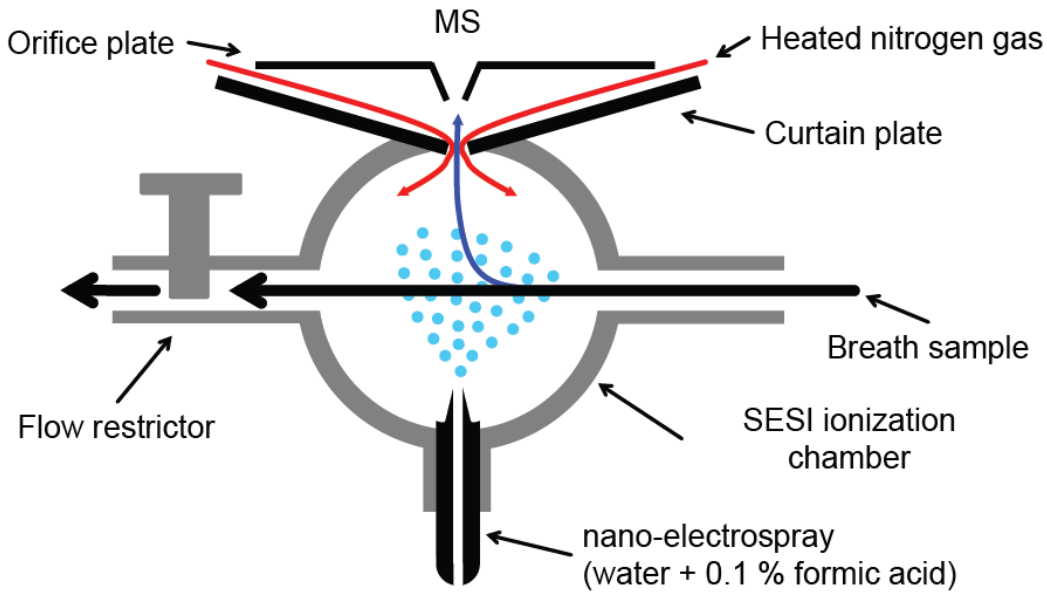

Figure E1. Scheme of the lab-built secondary electrospray ionization chamber coupled to a mass spectrometer to allow for the real-time breath analysis.

Figure E2

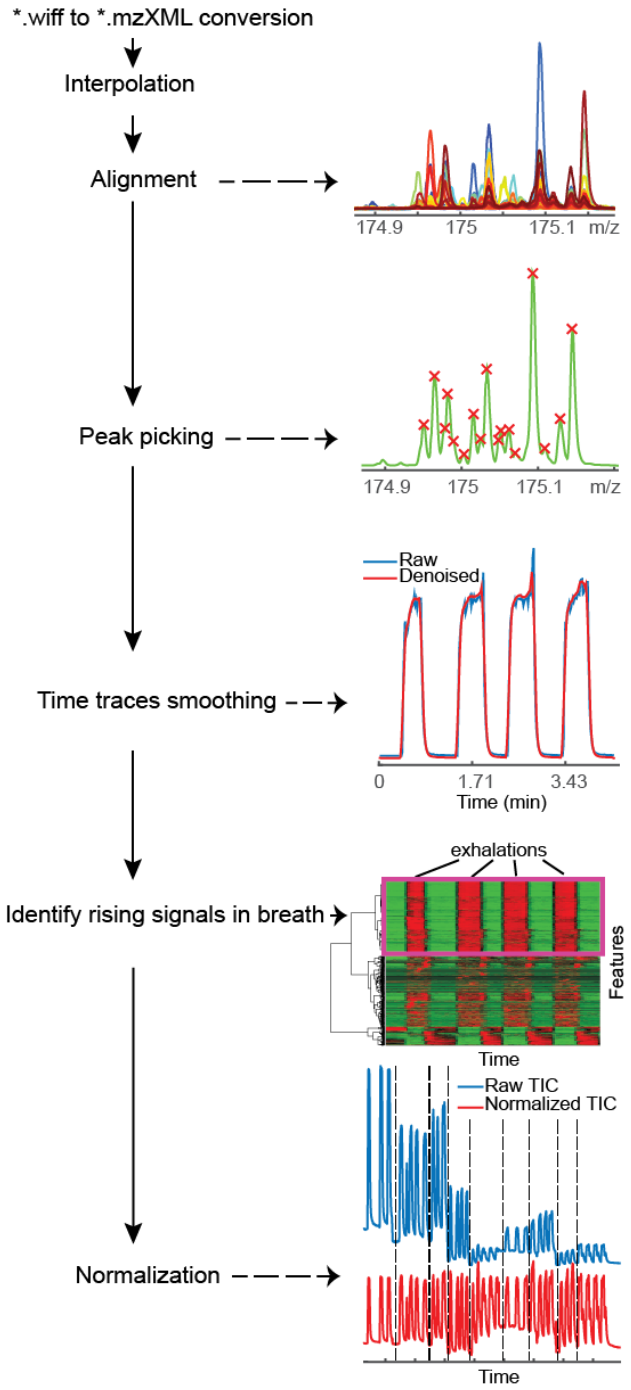

Figure E2. Workflow of mass spectra preprocessing.

Figure E3

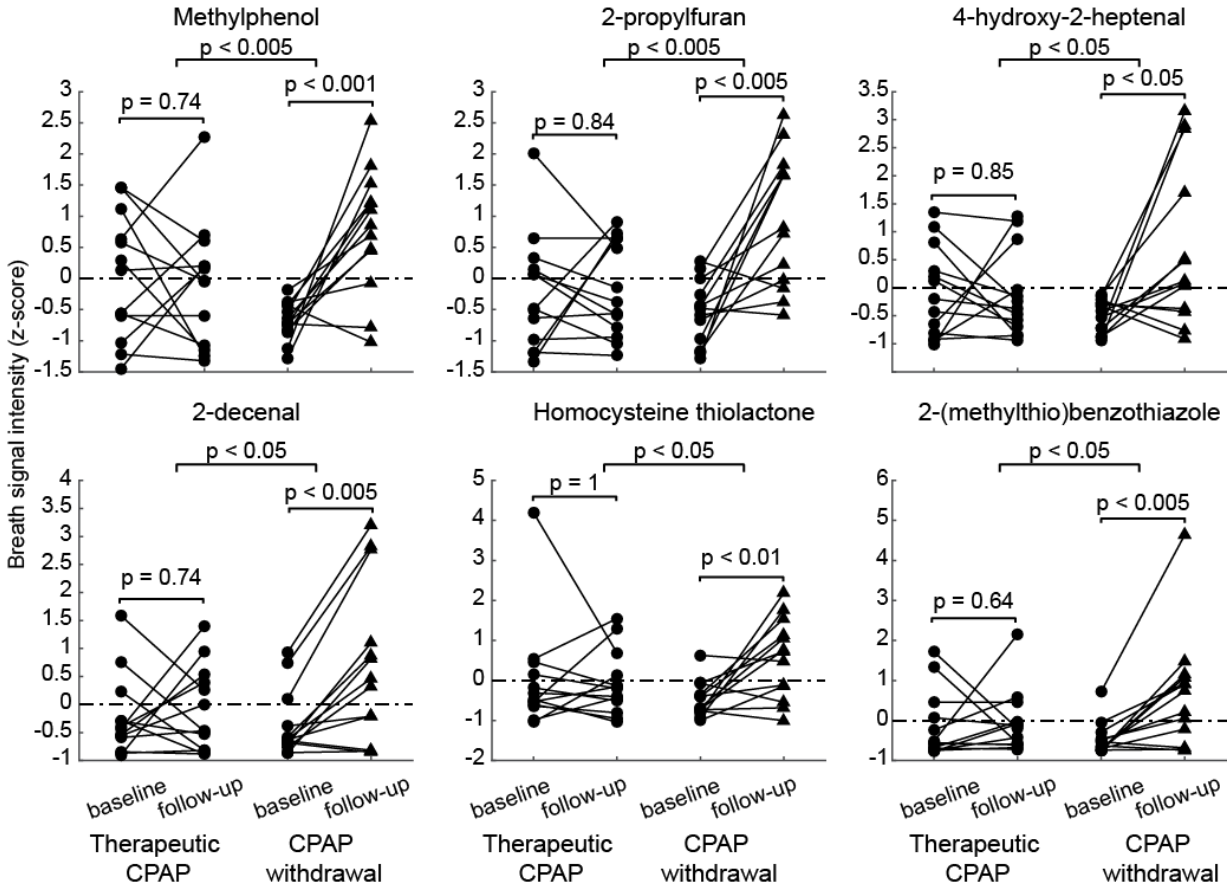

Figure E3. Changes of breath signal intensity of molecules significantly enhanced after CPAP withdrawal when compared to continuing CPAP (n=26); p-values for within and between-groups comparisons are quoted. See **Table E1** for details.

Figure E4

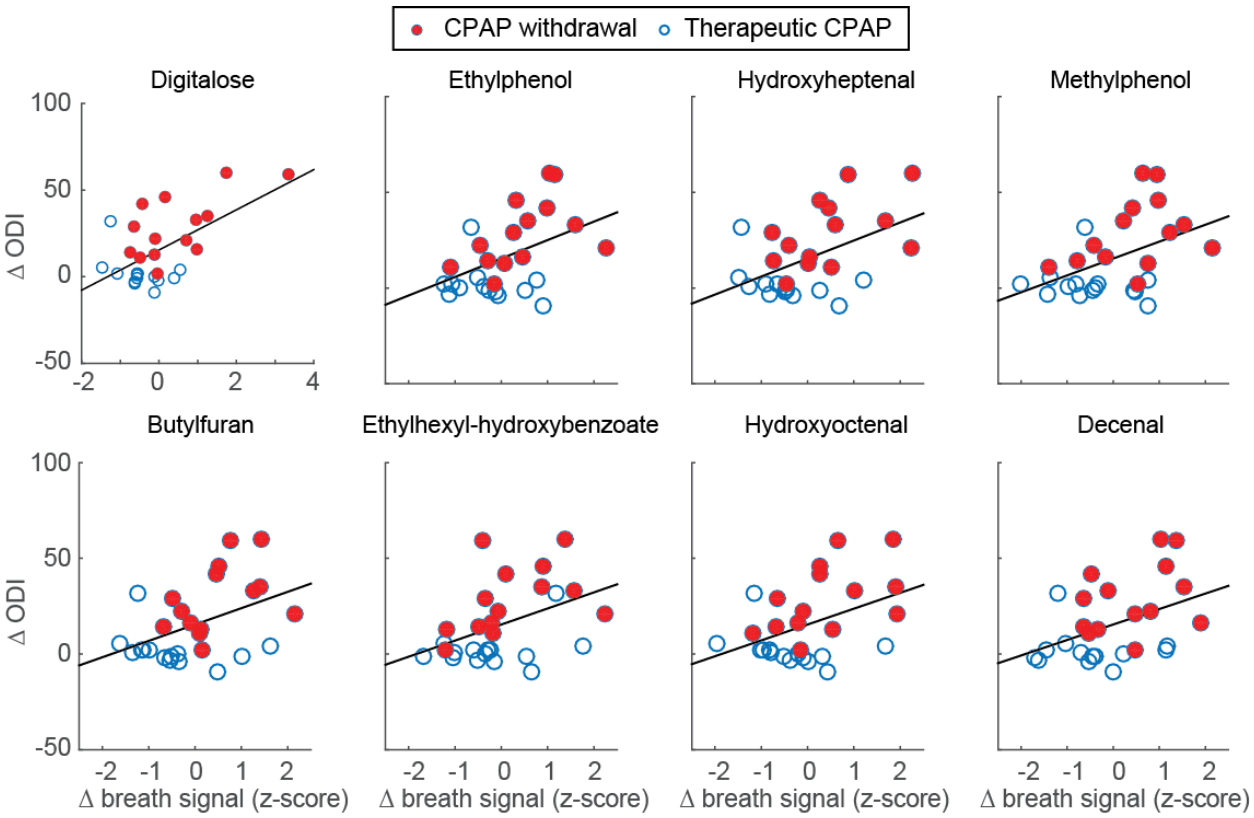

Figure E4. Selected molecules correlating with OSA severity (n=28). See **Table E2** for details.

Figure E5

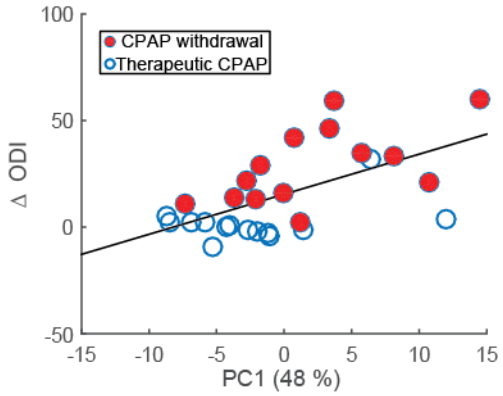

Figure E5. Change in (Δ) ODI vs. the first principal component score ($r = 0.59$; $p < 0.001$).

Figure E6

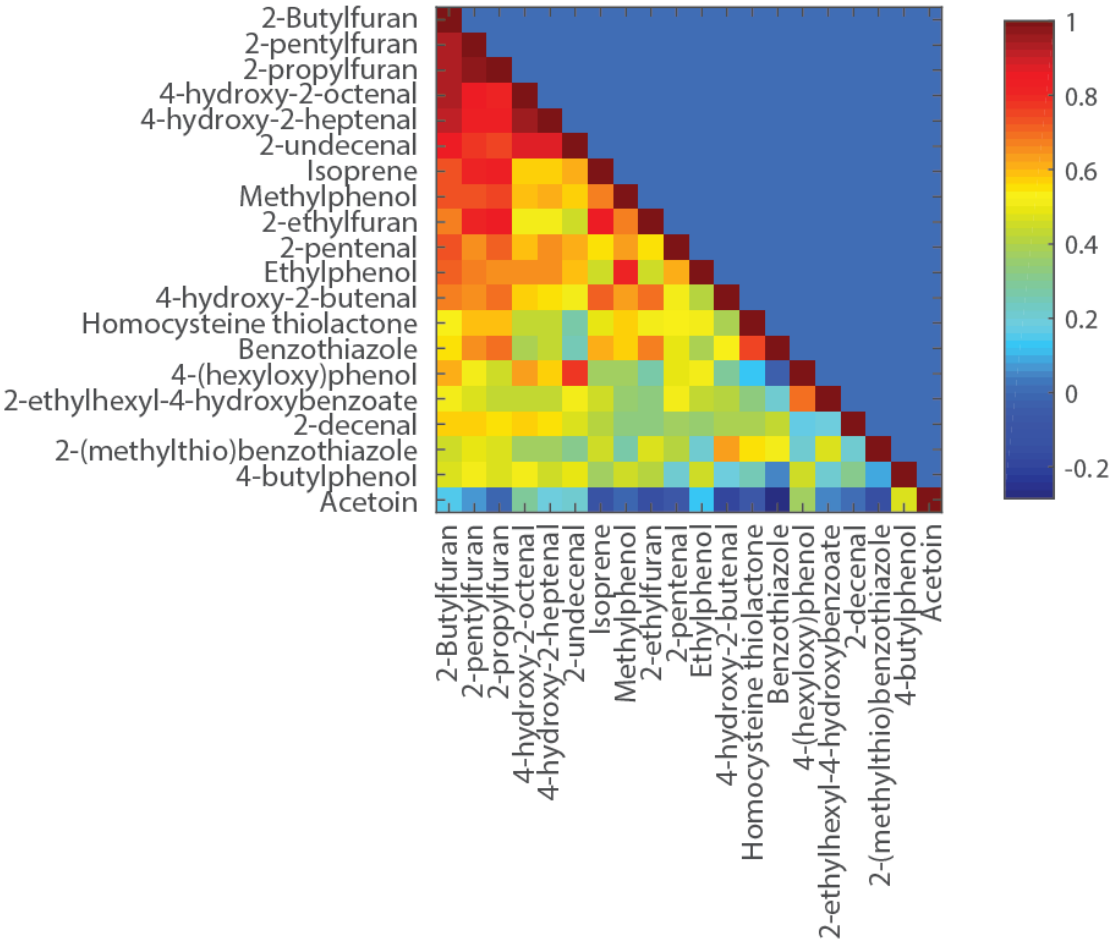

Figure E6. Heat-map of the correlation matrix for identified compounds in descending order of mean correlation from top to bottom. To reveal any latent association across the identified compounds, the correlation of each metabolite with all other metabolites was computed. A heat-map of the correlation matrix for all the identified compounds (the 20 with the highest degree of confidence) in descending order of mean correlation from top to bottom is shown. Note that the top ranked molecules are a series of furans and aldehydes. A further visualization of the connectivity network of the identified metabolites is shown in **Figure 3e**. Interconnected metabolites are based on their partial correlations (requiring $p < 0.01$).

E-REFERENCES

1. Kohler M, Stoewhas AC, Ayers L, et al. Effects of continuous positive airway pressure therapy withdrawal in patients with obstructive sleep apnea: a randomized controlled trial. American journal of respiratory and critical care medicine 2011;**184**(10):1192-9 doi: 10.1164/rccm.201106-0964OC[published Online First: Epub Date]|.
2. Rossi VA, Winter B, Rahman NM, et al. The effects of Provent on moderate to severe obstructive sleep apnoea during continuous positive airway pressure therapy withdrawal: A randomised controlled trial. Thorax 2013;**68**(9):854-59 doi: 10.1136/thoraxjnl-2013-203508[published Online First: Epub Date]|.
3. Schwarz EI, Schlatzer C, Stehli J, et al. The effects of short-term CPAP withdrawal on myocardial perfusion in OSA – A randomised placebo-controlled trial. Eur Respir J 2014 44:Suppl 58, 4664
4. Martinez-Lozano Sinues P, Meier L, Berchtold C, et al. Breath analysis in real time by mass spectrometry in chronic obstructive pulmonary disease. Respiration 2014;**87**(4):301-10 doi: 10.1159/000357785[published Online First: Epub Date]|.
5. Martinez-Lozano Sinues P, Tarokh L, Li X, et al. Circadian Variation of the Human Metabolome Captured by Real-Time Breath Analysis. PLoS ONE 2014;**9**(12):e114422 doi: 10.1371/journal.pone.0114422[published Online First: Epub Date]|.
6. Martinez-Lozano P, Fernandez de la Mora J. Direct analysis of fatty acid vapors in breath by electrospray ionization and atmospheric pressure ionization-mass spectrometry. Analytical chemistry 2008;**80**(21):8210-5 doi: 10.1021/ac801185e[published Online First: Epub Date]|.
7. Martínez-Lozano P, Fernández de la Mora J. Electrospray ionization of volatiles in breath. International Journal of Mass Spectrometry 2007;**265**(1):68-72
8. Martínez-Lozano P, Zingaro L, Finiguerra A, Cristoni S. Secondary electrospray ionization-mass spectrometry: breath study on a control group. J. Breath. Res. 2011;**5**(1):016002
9. Bean HD, Jiménez-Díaz J, Zhu J, Hill JE. Breathprints of model murine bacterial lung infections are linked with immune response. Eur. Respir. J. 2015;**45**(1):181-90 doi: 10.1183/09031936.00015814[published Online First: Epub Date]|.
10. Zhu J, Bean HD, Jiménez-Díaz J, Hill JE. Secondary electrospray ionization-mass spectrometry (SESI-MS) breathprinting of multiple bacterial lung pathogens, a mouse model study. Journal of applied physiology 2013 doi: 10.1152/japplphysiol.00099.2013[published Online First: Epub Date]|.
11. Wu C, Siems WF, Hill HH. Secondary Electrospray Ionization Ion Mobility Spectrometry/Mass Spectrometry of Illicit Drugs. Analytical chemistry 2000;**72**(2):396-403
12. Martinez-Lozano Sinues P, Zenobi R, Kohler M. Analysis of the exhalome: a diagnostic tool of the future. Chest 2013;**144**(3):746-9 doi: 10.1378/chest.13-1106[published Online First: Epub Date]|.
13. Chambers MC, Maclean B, Burke R, et al. A cross-platform toolkit for mass spectrometry and proteomics. Nat. Biotechnol. 2012;**30**(10):918-20 doi: http://www.nature.com/nbt/journal/v30/n10/abs/nbt.2377.html#supplementary-information[published Online First: Epub Date]|.
14. Keller BO, Sui J, Young AB, Whittal RM. Interferences and contaminants encountered in modern mass spectrometry. Anal. Chim. Acta 2008;**627**(1):71-81 doi: 10.1016/j.aca.2008.04.043[published Online First: Epub Date]|.

15. Riffenburgh RH. Chapter 15 - Managing Results of Analysis. In: Riffenburgh RH, ed. Statistics in Medicine (Third Edition). San Diego: Academic Press, 2012:325-43.
16. Storey JD. A direct approach to false discovery rates. J. Roy. Stat. Soc. Ser. B. (Stat. Method.) 2002;**64**(3):479-98 doi: 10.1111/1467-9868.00346[published Online First: Epub Date]|.
17. Breiman L. Random Forests. Mach. Learn. 2001;**45**(1):5-32 doi: 10.1023/A:1010933404324[published Online First: Epub Date]|.
18. Simon R, Radmacher MD, Dobbin K, McShane LM. Pitfalls in the use of DNA microarray data for diagnostic and prognostic classification. Journal of the National Cancer Institute 2003;**95**(1):14-8
19. Domingos P. MetaCost: a general method for making classifiers cost-sensitive. Proceedings of the fifth ACM SIGKDD international conference on Knowledge discovery and data mining. San Diego, California, USA: ACM, 1999:155-64.
20. Wolf S, Schmidt S, Müller-Hannemann M, Neumann S. In silico fragmentation for computer assisted identification of metabolite mass spectra. BMC Bioinformatics 2010;**11** doi: 10.1186/1471-2105-11-148[published Online First: Epub Date]|.
21. Horvath I, Hunt J, Barnes PJ, et al. Exhaled breath condensate: methodological recommendations and unresolved questions. Eur. Respir. J. 2005;**26**(3):523-48 doi: 10.1183/09031936.05.00029705[published Online First: Epub Date]|.
22. García-Gómez D, Martínez-Lozano Sinues P, Barrios-Collado C, Vidal-De-Miguel G, Gaugg M, Zenobi R. Identification of 2-alkenals, 4-hydroxy-2-alkenals, and 4-hydroxy-2,6-alkadienals in exhaled breath condensate by UHPLC-HRMS and in breath by real-time HRMS. Anal. Chem. 2015;**87**(5):3087-93 doi: 10.1021/ac504796p[published Online First: Epub Date]|.
23. Costello BdL, Amann A, Al-Kateb H, et al. A review of the volatiles from the healthy human body. Journal of breath research 2014;**8**(1):014001
24. Amann A, Costello Bde L, Miekisch W, et al. The human volatilome: volatile organic compounds (VOCs) in exhaled breath, skin emanations, urine, feces and saliva. J. Breath. Res. 2014;**8**(3):034001 doi: 10.1088/1752-7155/8/3/034001[published Online First: Epub Date]|.